1965

A study of the influence of shock waves on the stability of rock-bolt anchorage

Helmut W. Habenicht

A STUDY OF THE INFLUENCE OF SHOCK WAVES ON THE STABILITY OF ROCK-BOLT ANCHORAGE

BY

HELMUT W HABENICHT, 1937-

A

THESIS

submitted to the faculty of the

UNIVERSITY OF MISSOURI AT ROLLA

in partial fulfillment of the requirements for the

Degree of

MASTER OF SCIENCE IN MINING ENGINEERING

Rolla, Missouri

1965

Approved by

Richard L. Ash (advisor) James J. Scott

Ernest H. Roberts John B. Vaughan Jr.

ABSTRACT.

An experimental method was developed to compare strain data for rock and rock bolts when exposed to shock waves released by blasting. During a 32-day period of experimentation, one rock sensor and four rock-bolt sensors were observed simultaneously. By their placement in the side wall of a structurally stable drift, secondary static stresses were excluded. Bolt gage responses, then, could be considered to originate only from a decay of anchorage stability during static conditions or as a reaction to the vibrations.

Interpretation of test results indicated a distinct loss in bolt-strain during vibrations, accompanied by a smaller but steady loss of bolt-strain during static conditions. The strain losses were found related to the shock-source distance, the vibrational amplitudes in rock and bolts, and to the relative magnitude of vibrational energy in the two media.

ACKNOWLEDGEMENTS.

For the use of equipment of the Rock Mechanics Research Group, University of Missouri at Rolla, the author wants to express his gratitude to its Director, Dr. G. B. Clark. Furthermore, appreciation is due to Mr. Gus Kandaris for his help in solving technical problems of electronic nature. The writer is also most grateful to Messrs. G. W. Allen (Republic Steel Corporation), J. H. Scott (Bethlehem Steel Corporation), and D. R. Siljestrom (Colorado Fuel and Iron Corporation) for the supply of rock bolts used in the tests. In addition, the author wishes to especially acknowledge the guidance through his advisors, Professor R. L. Ash and Dr. J. J. Scott, during performance of this investigation.

TABLE OF CONTENTS

LIST OF ILLUSTRATIONS.

LIST OF TABLES.

LIST OF PLATES.

INTRODUCTION.

Rock-bolts are used to stabilize hard-rock structures by binding sections of rock to each other. They have played an essential role in mine-support for about the past 15 years. Because any load acting on the bolt will have to be transmitted through the anchor to the supporting rock, the placement of the bolt through the anchor-mechanism is of critical importance for successful application.

At present, knowledge of rock-bolt anchorage stability is extremely limited since little information on the subject has been published. This is especially true for vibrational loading conditions which have frequently been assumed to cause loosening of the anchorage. Uncertainty in this respect creates a risk in many cases of bolt application.

The present investigation was undertaken to gain knowledge of the influence of vibrations on the bolt-anchorage. Several recording techniques have been developed recently to define dynamic material-behavior. They have been utilized to develop an experimental method for the observation of bolts exposed to vibrations in natural mine rock and to produce experimental data that allowed quantitative correlation.

THE TESTING AND THEORETICAL CONSIDERATIONS OF ROCK BOLTING

A. Present Status of Investigations.

The development of a number of different bolt and anchor types (1, 2, 3, 4) has made it possible to utilize rock bolts in a variety of rock-types and support problems (2 through 13). An extensive literature search revealed that little effort has been made to study and analyze the anchorage mechanisms, although many publications deal extensively with bolting effects in mine structures.

In consideration of test methods and pertinent equipment, anchorage response to dynamic loads, e.g., those from blasting and similar vibrational or impact-type stressing, has received only slight attention by investigators. The main concern of work done has not gone beyond static bolt-load capacity and static anchorage-characteristics. For this purpose, several testing methods were developed that allow experimental determination of index data. One of these was described by Stefanko (1) as a dynamic test, but should be more appropriately termed a Pull Test.

To conduct a Pull Test, a bolt is pulled by an axial force until its measured displacement becomes excessive (i.e., when either a complete, or a certain defined anchor slip takes place without a corresponding load increase), or until the bolt material fails. The force measured at this point is taken as characteristic for the anchorage capacity. The relative simplicity of the equipment used and performance achieved has made it frequently used, being recommended as a standard method by the Committee on Roof Action of the American Mining Congress (14). The method's practical importance lies in the ability

to test anchorage efficiency as well as the influence of shell design and rock-material characteristics.

A second test method, also frequently employed, involves observation of the load loss of a bolt over a relatively long period of time, details for the performance of which are described in a number of publications (1, 3, 9, 10). The test considers the fact that shortly after installation, bolts exhibit a "bleed off" of load, presumably caused by slippage of the anchor due to deformation of the rock material when exposed to high stressing. The deformation characteristics of rock materials, the forces involved, and the size and design of bolt anchors strongly influence the test results which are presented in the form of a plot of load versus time. Since observations of the subsequent long term-behavior are of no less importance, especially for determining the relative stability of permanent-support structures, it is advantageous to combine this test with other types of measurements. The latter measurements would involve those of convergence, roof sag, swell, etc., which can contribute much to establishing a more complete picture of the structural performance of an entire rock-bolting system.

As load-indicating devices, relatively slow-response load cells are used most often in experiments. However, other devices might also be applied. For example, a variety of bonded, electric resistance-wire strain-gages are available for measuring strains induced in materials.

Strain gages exhibit advantages over many of the other load measuring devices because of their high sensitivity and immediate response to strain changes. They are bonded directly to the investigated member, require little space, and exert practically no interference with the reaction of the tested member. Strain gages have been most successful

in measuring dynamic responses to vibrational and impact stressing. Therefore, one would assume they could be used as an appropriate device to investigate the anchorage stability of bolts when they are exposed to dynamic loads.

B. Rock Bolt Mechanisms.

1. Purposes and Functioning of Rock Bolting.

Rock bolts are applied in mine support to prevent strata separation and roof sag, to increase the effective strength of roof strata and rock zones immediately surrounding openings, to stabilize pillars and walls, to prevent rock falls, and to suspend or hold support-members and machine elements in place. The basic principles of application are outlined in the various publications mentioned earlier and need not be discussed in detail. However, the success achieved in all types of bolting is basically dependent on the degree with which the acting load can be transmitted to the bolt head, then along the bolt shank to the anchor elements, and lastly, into the rock at the anchor site (Figure 1).

For the two types of bolts customarily used, e.g., wedge and expansion-shell, the element with the most uncertain function is the anchor. Wedge-type anchors establish coupling with the borehole wall by the relative movement of the axially slotted end of the bolt against a simple wedge positioned in the slot at the end of the borehole. As the bolt is driven axially into the borehole, the wedge is forced into the slot, separating the two half-sections of the bolt-end and compressing them against the borehole wall. A strong joint is formed that can be released only by material failure. Expansion-shell type anchors also function by wedge action but as a result of bolt rotation. The

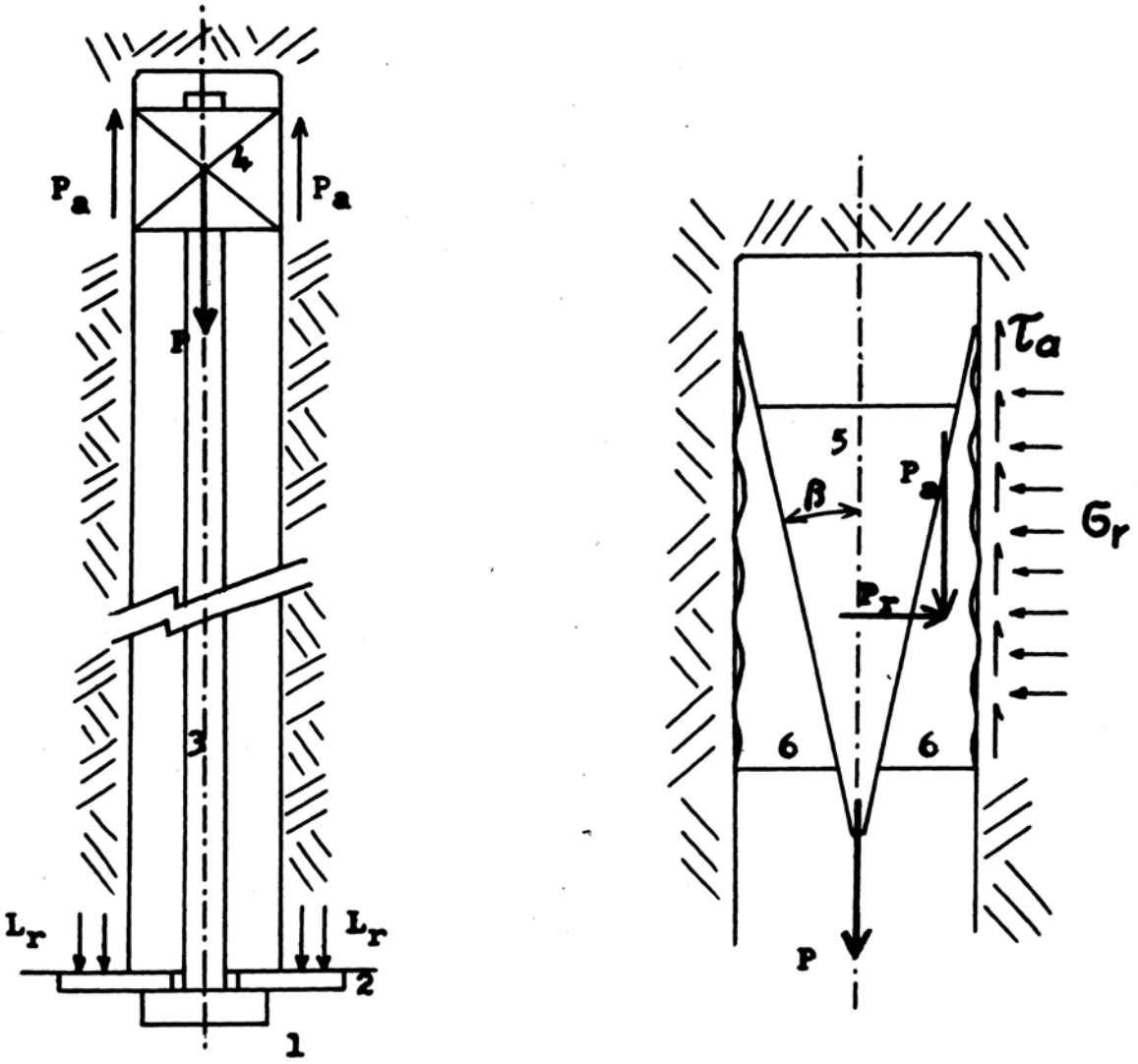

1...BOLT HEAD

2...CARRIER PLATE

3...BOLT SHANK

4...ANCHOR

5...WEDGE

6...LEAF

(a) (b)

Figure 1. Load and Stress Conditions Around Bolt (a), and Anchor (b).

wedge and an outer expansion-shell form the primary anchorage elements. The wedges are equipped with an axial bore that is threaded, which in turn, is screwed on the threaded end of the bolt. As the bolt is rotated, the wedge moves axially toward the head of the bolt, at the same time expanding the leaves of the constraining shell. The shell is prevented from axial movement by various design techniques (1, 2, 6, 8, 10, 11, 14, etc.). Serrations on the outside of shell leaves of various forms are manufactured to permit applications in a wide range of rock types.

For all kinds of anchors, stress interactions with the rock material are quite complex, and investigations of anchorage behavior would require complicated analysis techniques. However, of the various component parts of a bolt, the shank represents an element of such singular importance to the mechanism that the tension acting in it could be taken as possibly characteristic of the performance of the entire bolt under load. One would expect that a change in bolt tension results most probably from anchorage disturbances, if the acting load at the bolt-head remained primarily unchanged.

2. The Mechanics of Anchorage.

To allow deeper insight into anchorage-stability conditions when using expansion-shell type anchors, an evaluation of forces and stresses induced into the rock by the anchor would be fundamental (Fig. 1). According to equations developed from basic laws of mechanics by De La Cruz (18), the radial force, P_r, acting from an anchor into the rock can be expressed as a function of the axial force, P, acting along the bolt shank, and of the design characteristics of the anchor elements μ, w and s, as follows (see Appendix I for a complete list of symbols):

$$P_r = P(1 - \mu_w s) / n(\mu_w + s). \quad 1.$$

In turn, the magnitudes of the axial force in the anchor, P_a, and the counter-acting normal and shear stresses in the rock, σ_r and τ_a, respectively, would be related to the radial force, P_r, simply as follows:

$$P_a = P_r \mu_r, \quad 2.$$

$$\sigma_r = - P_r/A, \quad 3.$$

$$\tau_a = P_r \mu_r / A, \text{ and} \quad 4.$$

$$\tau_a = -\sigma_r \mu_r. \quad 5.$$

According to the equations, a force acting axially along the bolt could be translated directly into terms of stress created in the rock at the anchor site. The stresses could be determined for any given set of conditions. For example, let it be assumed that a Pattin D-3 two-leaf expansion-shell anchor were used. In this case, the anchor specifications would be n = 2, $\mu_w = 0.25$, $\mu_r = 0.35$, s = 0.14, and A = 0.49 $in.^2$, the latter value of which would be where only the edges of serrations make contact with the rock. If the applied load, P, were 4000 lb., then from Equations 1, 3, and 5, the stresses in the rock could be calculated as follows:

$$\sigma_r = -P_r/A = - \left[P(1-\mu_w s)\right] / \left[nA\ (\mu_w + s)\right],$$

and $$\sigma_r = - \left[4{,}000(1 - 0.25 \times 0.14)\right] / \left[2 \times 0.49\ (0.25 + 0.14)\right],$$

or $$\sigma_r = -10{,}000 \text{ psi}.$$

Also, $$\tau_a = -\sigma_r \mu_r = - (-10{,}000)(0.35),$$

or $$\tau_a = 3{,}500 \text{ psi}.$$

Logically, as the area, A, of contact increases, the stresses would be expected to decrease proportionately. Also, on the assumption the elastic limits of the bolt materials and the rock are not exceeded, a

strain observed in the bolt shank could be translated directly into strain resulting in the rock.

Since the same applied load exerts stresses to both the anchor in the hole and on the carrier plate at the bolt-head, the stress conditions at the plate location are also of interest. For example, if one were to assume a 6-inch square carrier-plate in contact with the rock for only 10 per cent of its area, due to roughness of the rock's surface, then σ_r would be only 1100 psi, since $\sigma_r = -P/A = -(4000)/(0.10 \times 6 \times 6)$. As also for the anchor, greater contact area at the carrier plate would reduce the stress magnitudes in the rock.

The stresses at the anchor site determined by Equations 1 through 5 assume that the rock provides sufficient strength in the elastic region to withstand the contact stresses and to hold the anchor in place without suffering deformation. Since the calculated stresses represent average stress values, peak stresses much higher than those no doubt would occur. Because rocks are composed of several minerals with varying strengths, it would be very unlikely that under such conditions no deformation would occur. In addition, the stresses at the anchor contact could be of magnitudes that, for many cases, would be close to or above the rock strength. Therefore, the conclusion could be drawn that the effective stresses at the anchor site normally would be far more critical than those at the bolt head. This consideration supports the frequent explanation that failure in rock-bolt action results at the anchor rather than at other points.

3. Effects from Vibrational Stressing.

In addition to static stresses, rock bolts often are subjected to

vibrational types of stressing. Strains from this type of stress could be induced by impact loads such as those from blasting. Their influence on the anchorage mechanisms is not known but it has long been thought that the effects could be detrimental to the extent that anchorage stability might be disturbed (16,17,18).

Measurement of strains in rock from stresses produced from impact loads has been successfully accomplished by Duvall, Obert, Quan, and many others (19,20,21,22). It was shown that although very high strains were produced near the source of impact, strains in the rock at distance were greatly decreased in magnitude. This was because the stresses were weakened by energy absorption, divergence, and scattering effects as they were propagated out and away from the source.

Unlike the effects produced from statically imposed loads, the resulting strains from impact stressing exhibit a vibratory character. The action is similar to that from seismic waves, with the energy being transmitted in a form consisting of a series of strain pulses. Of the kinds of strain pulses, the compressional pulse is generally stronger and travels the faster, as it is from one and one-half to two times the velocity of the transverse or shear pulse. Thus, the compressional pulses would be the first to encounter any point of contact between the rock and a bolt, to be followed later by the transverse strain pulses.

Seismic pulses characteristically are reflected and refracted at materials' interfaces, scattering the original energy by generating new pulses at each discontinuity (23). Of the original pulse-energy, a portion is transmitted into the bolt at the points of contact, part is reflected back through the rock (Fig. 2), and some may be consumed in the form of work that may occur. Work lost at interfaces could go into

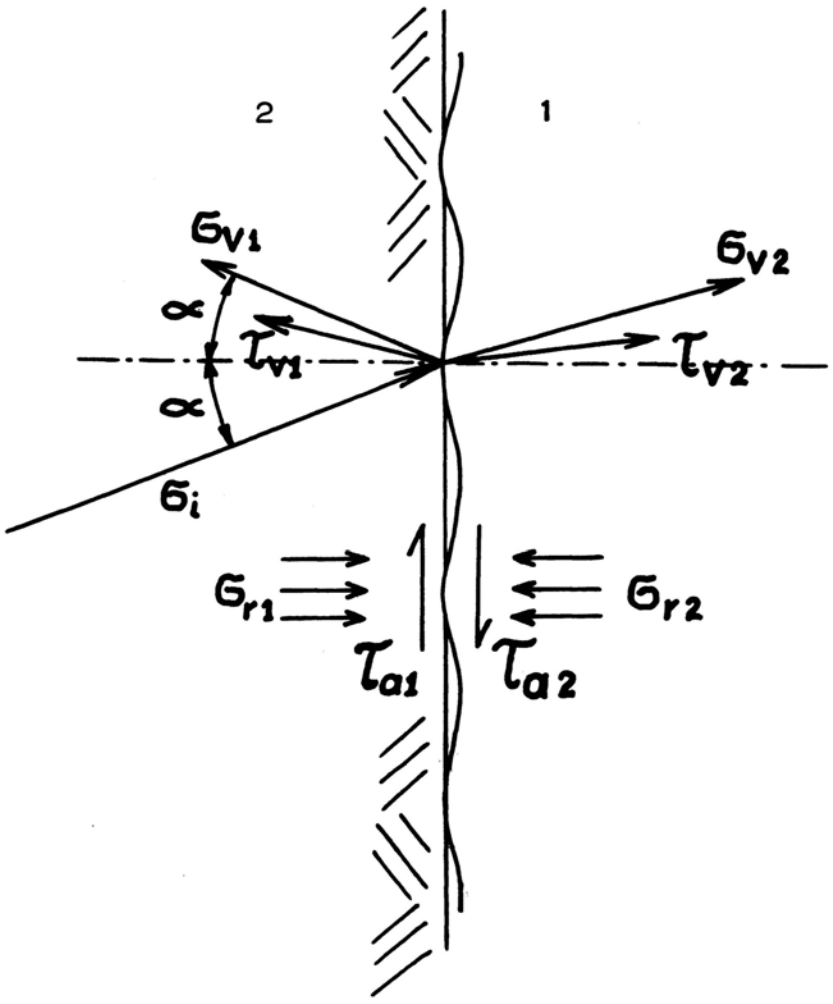

1 ..... ANCHOR SHELL

2 ..... ROCK

Figure 2. Schematic of Wave Dispersion at the Shell to Rock Interface.

deformation and fracturing of the mineral components making up the rock. Because rock bolts provide basically only two points of contact with rock, i.e., at the anchor and at the carrier plate, high strain conditions most likely would be developed at both those locations. The vibrational strain would be superimposed on the static strains already existing at the bolt site, so that the addition to the existing strain condition could cause rock rupture or deformation not previously experienced.

As one would suppose, a mathematical analysis of conditions at the anchorage points would be extremely complex, and simple engineering solutions at the present state seem almost impossible. Since it is not known of what nature the vibratory behavior of rock and shell at their contact might be, it appears feasible to begin an investigation of stability conditions by experimental observation of such phenomena. Providing the anchor is in intimate contact with the rock, vibrational energy introduced into the anchor should be transmitted to the shank. According to this assumption, one could postulate that strain changes occurring in the shank of a bolt result from processes going on in the rock and at the rock-to anchor interface. Thus, their magnitude and character can be expected to contain some indication of effects occurring at the points of contact.

EXPERIMENTAL WORK.

A. Instrumentation.

In consideration of the reports on the successful observation of rock vibrations by Quan (21), the U.S. Bureau of Mines (20), and by the recommendations for the use of electric resistance-wire strain-gages (9, 10, 22), a technique was developed for observing the simultaneous vibrational behaviour of rock bolts. It was designed to utilize equipment proven to be reasonably reliable under conditions of the test site and to allow fast operation with high sensitivity in data production. In these respects, full advantage was taken of equipment designed by Quan during similar investigations at the same test site, with certain modifications incorporated in the basic circuitry to accomodate more channels and rock-bolt strain measurements. The complete test equipment, as shown schematically in Fig. 6, was composed of four basic units: a set of test rock-bolts, a strain sensing and transducing system, photographic cameras for data recording, and a shock initiation source with appropriate firing and synchronizing trigger-circuit.

1. Test Rock-Bolts.

In order to provide results with the most practical value, standard expansion-shell type rock-bolts were selected, with dimensions in the range of those most frequently employed in industry (see Appendix III). A special steel disc was attached between the bolt heads and the carrier plates to decrease frictional resistance to rotation at their contact. This arrangement was used to increase the efficiency of torque transmission to the thread during installation. The bolts were further equipped with strain gages as described below.

2. Strain Sensing and Transducing System.

a. Strain-Sensors. To permit observation of both static and dynamic strains in bolts, and also in the surrounding rock, two types of sensor units were built:

(1) Rock-Sensors. Based on reports describing similar work (20,21,27), the wave form to be observed was assumed to be a plane wave. It was decided to record only the longitudinal component, since development of transversal vibrations was not expected. Thus, it was considered satisfactory to mount a single strain gage in the rock medium. To assure uniformity of gage properties throughout the experiment, SR-4 type isoelastic resistance-wire gages were used. They were bonded to the base plane of a cylindrical core extracted from the rock at the test site. The procedure followed in manufacturing of the units was described in detail by Quan (21). The design of the rock-sensor and the associated electrical transducer-circuit are illustrated in Fig. 3.

(2) Bolt-Sensors. Difficulties had to be overcome in the proper placement of strain-gages on the bolts and in the building of attendant circuitry (see Appendix II). The design found to be the most reliable was similar to that developed by Stefanko and De La Cruz (1). At each bolt four strain-gages were installed to function as one sensor unit, whereby gages were grouped into the circuit of a Wheatstone Bridge (Fig. 5). Because of the close arrangement of the sensitive elements, disturbing influences were excluded to a high extent, e.g., electronic noise, humidity, temperature, capacity variations, and differences in conductor length. The gages were bonded with commercial du Pont Duco Household Cement to a properly prepared space on the surface of the bolt shanks. They were protected from humidity by

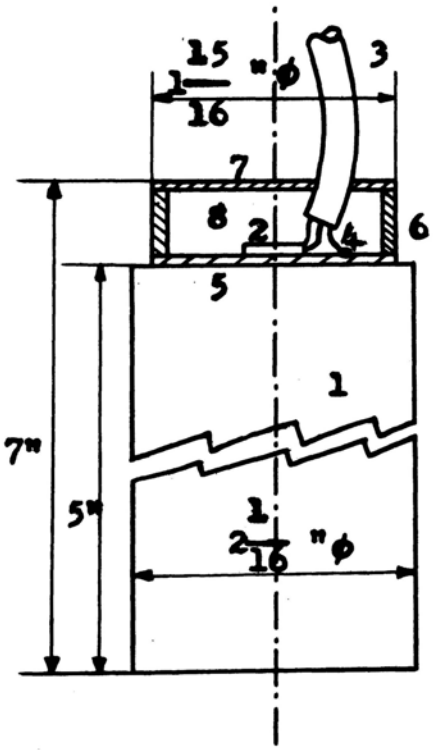

1 ... ROCK CORE
2 ... STRAIN GAGE
3 ... CONDUCTOR CABLE
4 ... SHIELD
5 ... COPPER FOIL
6 ... BRASS CYLINDER
7 ... COPPER FOIL
8 ... EPOXY FILLING

(a) Composition of Rock-Sensor.

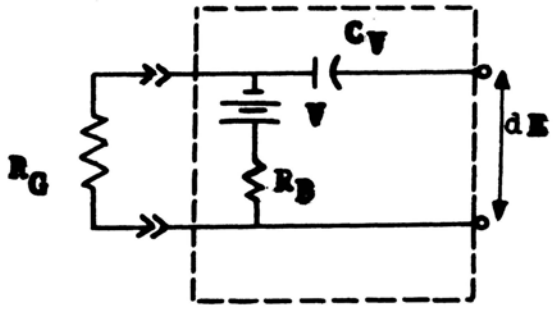

dE ... OUTPUT-SIGNAL
R_G ... GAGE RESISTANCE
V .... D.C. POWER SUPPLY
R_B ... BALLAST RESISTOR
C_V ... COUPLING CONDENSOR

(b) Electrical Transducer Circuit.

Figure 3. Rock Sensor.

the application of an epoxy coating and shielded electronically by a wrapping of copper foil.

Because of the geometric configuration (Fig. 5, Fig. 6), simultaneous compensation of differences in temperature and bending strains was possible. Positioning of the gage units at a distance of 12.0 inches from the bolt head was felt adequate for the purpose of providing enough space for coiling a sufficient length of conductor cable between gages and the bolt head. Coiling of the cable around the shank prior to installation was necessary to provide sufficient slack for it to unwind during rotation of the bolt.

b. Conductor Cables. Nine feet long, shielded four-conductor cables served as permanent conductors at each bolt. They were clamped with wire to the bolt shank on one end and equipped with a four-pin male cable-connector on the other end, to fit the receptacles on the strain indicator. The cable shielding was welded to the bolt shank for proper grounding.

For the connection between the bolt-gage cables and the recording instruments, which were installed in a surface building at some distance from the immediate test site, five 250-ft. long shielded two-conductor cables were used. Because of the different electrotechnical role of the gage bridge in the oscilloscope circuitry, only two contacts to the gage bridge of a bolt were necessary. Thus, the positive and the negative conductors of the cables were connected to only the power contacts, B and C, of a gage bridge. To provide a completely shielded circuit, the cable shield was connected at one end to the bolt shank and at its other end to the shell of the cable connector.

To match the male four-pin connector at the bolt-cables, the 250-ft. cables were equipped with corresponding female four-pin connectors

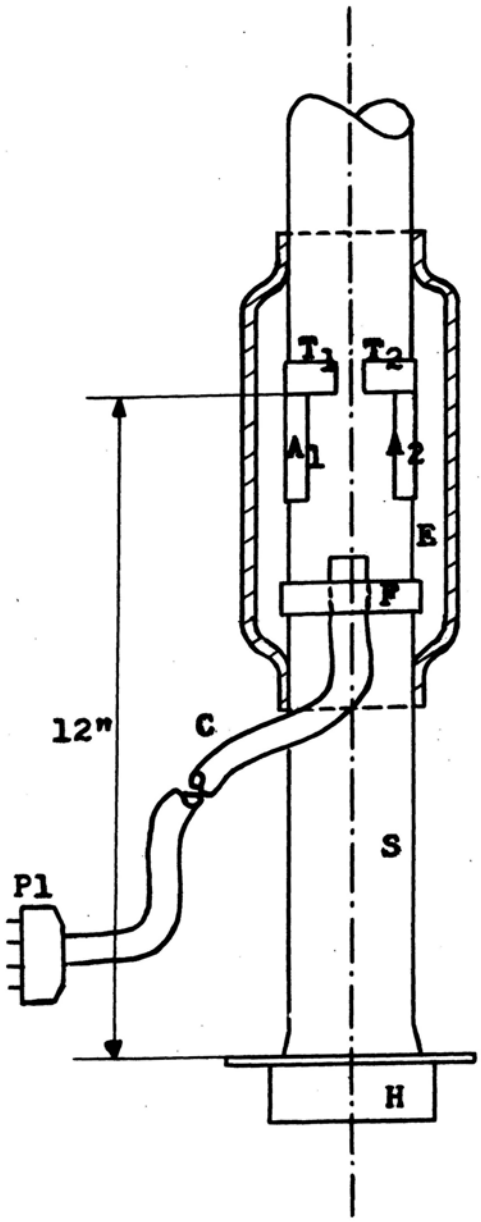

H ..... BOLT HEAD

S ..... BOLT SHANK

A_1,A_2.. ACTIVE GAGES

T_1,T_2.. TEMPERATURE COMPENSATING GAGES

Sd .... COPPER-FOIL SHIELD

E ..... EPOXY COATING

F ..... CABLE FIXATION

C ..... FOUR-CONDUCTOR CABLE

Pl .... FOUR-PIN PLUG

Figure 4. Composition of Bolt-Sensor.

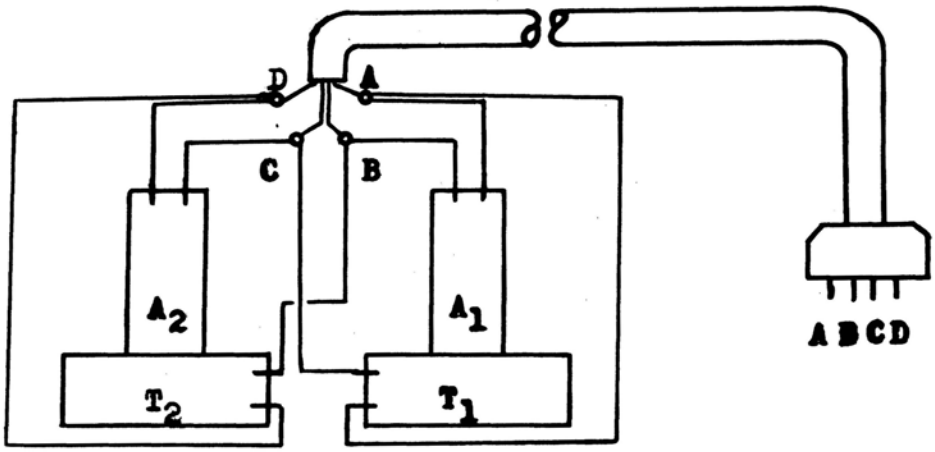

A_1, A_2 ... ACTIVE GAGES

T_1, T_2 ... TEMPERATURE COMPENSATING GAGES

B - C ... POWER SUPPLY FOR BRIDGE

A - D ... STRAIN METER IN BRIDGE OUTPUT

(a) Position and Wiring of Bolt-Gages.

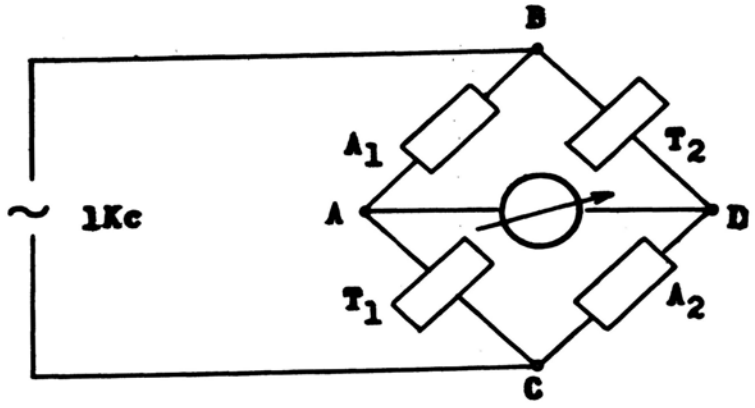

(b) Wiring Diagram of Bolt-Gages for Static-Strain Readings.

Figure 5. Bolt-Gage Arrangement.

of which only pins B and C were soldered to the two conductors of the cable. On the recording-equipment end of the cables three-pin microphone connectors were mounted to fit the receptacles of the transducer input units. In the case of the rock-sensors, the same type of two-conductor cables was used. However, three-pin microphone connectors were fixed on both ends, in much the same manner as was done in Quan's experiments (21).

c. Transducer Input Units and Preamplifiers. Before the output from the bolt and rock sensors could be fed into the oscilloscopes, they had to pass through a signal modifying system consisting of transducer input units and preamplifiers. The role of the transducer input units was two-fold: to supply the strain gages with a rated amount of current, which had to carry the signal output, and to transform the signal consisting of a resistance change, ΔR, into a voltage change, dE, for delivery to the preamplifiers. Five input units, Tektronix Brand, were employed (Fig. 6 and Plate I). Their operating power was provided by 90-volt dry-cell radio batteries, from which a current of 25 ma was fed into each strain-gage circuit.

More for the purpose of noise filtration and control of band width than to amplify the signals, one low-level preamplifier (Tectronix Type 122) was connected in the circuit between the transducer input units and the oscilloscopes. They were operated by D.C. power, utilizing 6-volt automobile batteries for the A supply (filaments), 135-volt radio batteries for the B supply (plates), and 90-volt radio batteries for the C supply (bias).

Although adequate oscilloscope sensitivity was available, the preamplifiers were operated on a 100-fold amplification to exploit their

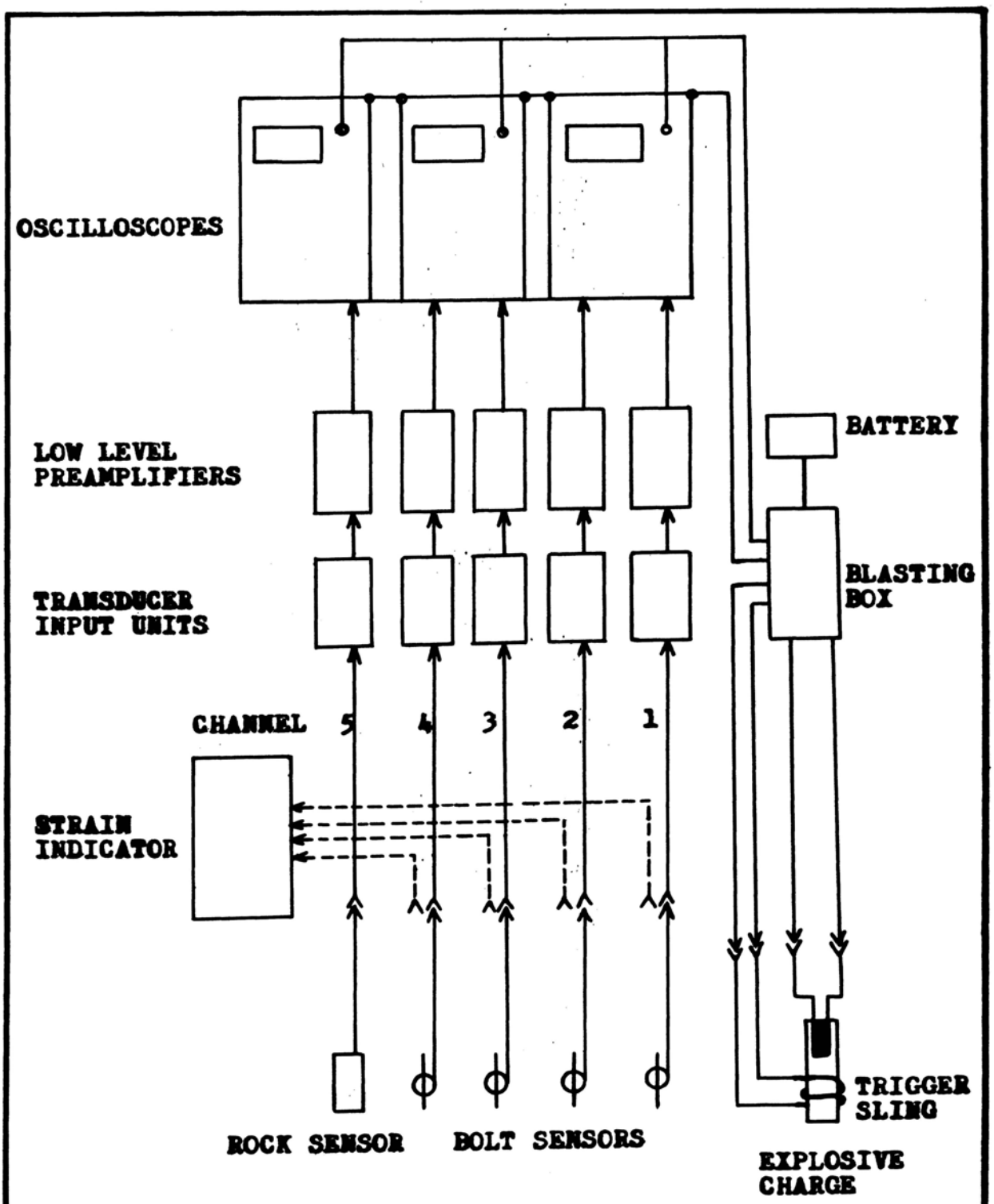

Figure 6. Schematic Diagram of Instrumentation System.

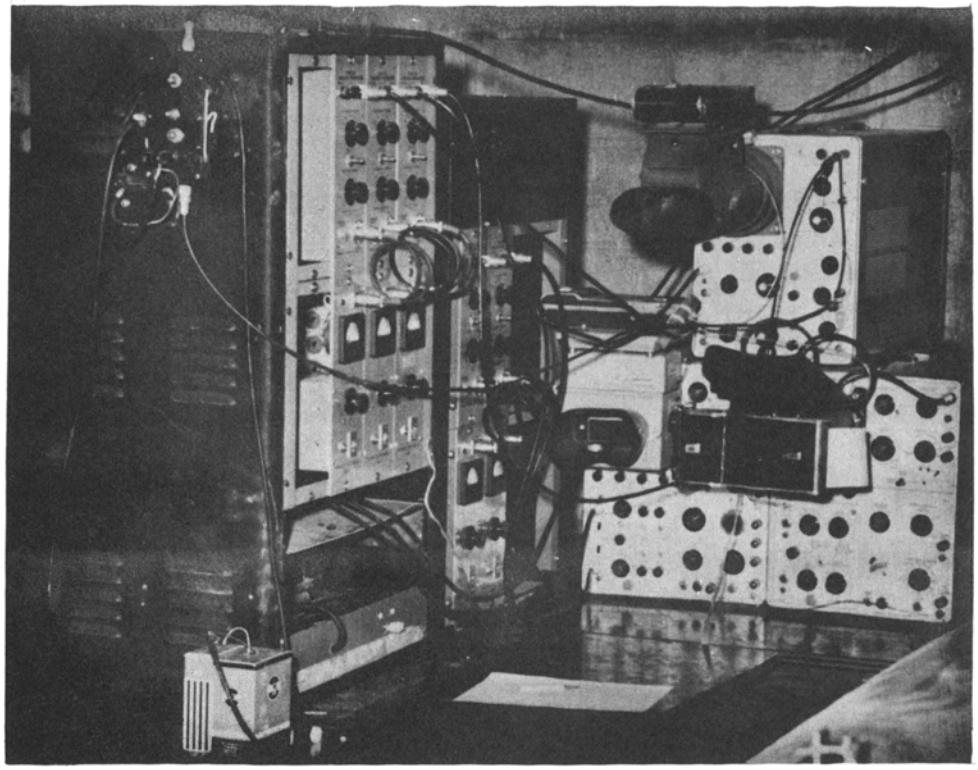

PLATE I

Recording Equipment at the Observation Stand.

(Transducer Input Units and Preamplifiers in Steel-Closets at Left. Oscilloscopes and Cameras at Right.)

full filtration capacity. Bandwidths were set between 10,000 and 80 cycles, since this range was expected to contain most of strain wave frequencies (21). The amplifier outputs were fed directly into the oscilloscopes.

d. Oscilloscopes. Three cathode-ray oscilloscopes were available for simultaneous observation of individual strain-gage signals. They included Tectronix Types 533, 502, and 535 A. The latter two were equipped with dual-trace plug-in units, so that a total of five traces was available for simultaneous use. A number was assigned to each trace, together with its corresponding transducing circuit and strain sensor, in order to designate each of the branches as a channel. Power for the oscilloscopes was supplied from a 110-volt power source. Sensitivity ranges and sweep rates of the oscilloscopes were similar to the ones described at length by Quan (21) for the Tectronix Type 502.

e. Static-Strain Indicator. For observing the static loads present in the installed rock-bolts, a Hathaway Model SR-20C strain indicator was used. It contained 12 channels for simultaneous use in the observation of several strain-gages. It functioned on the basis of a 1-kc carrier wave, whereby disturbances from electronic noise were excluded to an extent below the instrument's accuracy. For the particular type of strain-gages used, a compensating 158-ohm resistor was inserted in the rear panel, according to the Instruction Manual. A sensitivity of $\pm$ 0.1 microstrain in the range from 0 to 1,000 microstrain and of $\pm$ 10 microstrain in the range of 1,000 to 20,000 microstrain assured high accuracy in the observation of bolt behavior.

3. Photographic Recorders.

Because of the very short time interval of wave passage through

the sensors and the need for permanent records, visual observation of trace developments on the oscilloscope screens had to be excluded from consideration. Three Polariod cameras, each mounted on one of the oscilloscope screens recorded the events on Type 47 Polaroid film. The high sensitivity and speed of the film allowed inspection of pictures within 15 seconds after exposure, which in turn permitted prompt adjustment of testing procedures when required.

4. Shock Source and Triggering-Circuitry.

Since blasting is the most frequent cause of vibrations in mining operations, single unit-charges of explosive were selected as a standard for vibration generation. Due to the need for a relative large number of tests under reasonably unchanged conditions, the explosive size had to be restricted so that a minimum of fracturing damage would result to the rock. Therefore, each explosive unit was made up of two 1-1/4 x 8-inch cartridges of Atlas Gelodyn No. 3, containing a total charge weight of 0.9 lb.

Atlas instantaneous No. 6 electric blasting caps were used for the initiation of charges. A D.C. firing current was supplied from a condensor-type blasting box mounted on the oscilloscope stand (Fig. 6 and Plate I). To synchronize the sweep of the oscilloscope traces with the detonation of each charge, a wire sling was taped around the primer cartridge. A -90-Volt potential was applied to this sling for the purpose of blocking the trigger system of the oscilloscopes. Rupture of the sling by the explosive's detonation removed the blocking voltage and released the sweep of the oscilloscope beams. The voltage for the trigger system was supplied from the condensor box.

B. Test Procedure.

1. Concept of Experimentation.

In principle, the concept of the experimental investigation was to find from a series of rock bolts installed in natural mine rock whether or not, and to what extent, bolt tensions would be influenced when the bolts were exposed repeatedly to shock waves released by blasting. For this purpose, it was felt necessary to simultaneously observe the extent of rock vibration through the strain-gage equipped rock-core grouted into the rock. A comparison of the two types of data, from bolt and rock vibration, should lead to quantitative conclusions for relationships between vibrational characteristics, geometric configuration, and anchorage stability.

2. Selection of the Test Site.

It was intended that influences from structural conditions on data to be recorded, e.g., from roof sag, strata separation, load transposition, etc., would be minimized by mounting the bolts in a mechanically stable section of underground rock. With regard to the additional advantages of easy access and ventilation, as well as of constant temperature conditions (temperature readings remained in the range between 60.5 and 61.0°F), a part of the NE-drift in the Experimental-Mine of the University of Missouri at Rolla was chosen (Fig. 7 and Table 1). Bolts and rock-sensors were installed in the side wall of this drift (Plate II). A further reason for selecting of this particular location was the proximity of the test site recently used by C. K. Quan, where rock sensors were still in place. It was intended to recheck the functioning of these devices and to compare their output with that of the sensors used in this investigation.

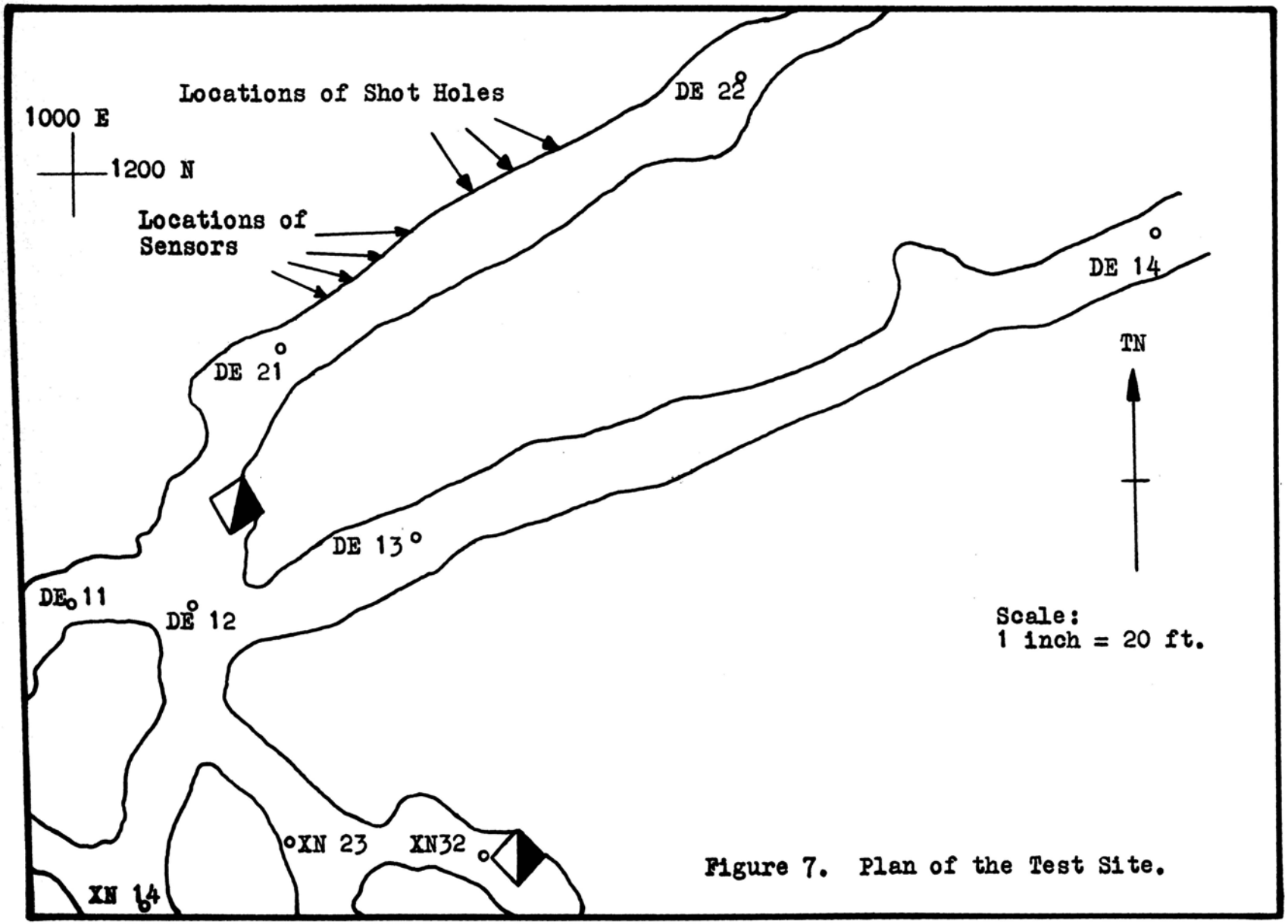

Figure 7. Plan of the Test Site.

Table 1.

Physical and Petrographic Properties of the Mine Rock (21).

Physical Properties:	
Specific Gravity	2.8 gm/cc
Porosity	13.0 %
Ratio of Absorption	5.3
Weight per cu. ft.	152.2 lb
Tensile Strength	220.0 psi
Crushing Strength	8476.7 psi (on bed) 9161.0 psi (on edge)
Modulus of Elasticity	3.5×10^6 psi
Modulus of Rupture	1,000 psi
Longitudinal Velocity	17,300 ft/sec
Petrographic Composition (Average):	
Dolomite	65 %
Calcite	20 %
Quartz, Chert, Limonite, Pyrite, Clay	15 %

3. Installation of the Rock-Sensor.

After response of the rock-sensor was checked in the Laboratory, a NX-size borehole of 5-ft. depth was drilled slightly inclined downward into the side wall of the drift. For installation, the device was placed first into the bottom of the hole and then rotated into a position, such that the mounted strain-gage was most sensitive to horizontal strain components. A steel pipe was then pushed into the hole beside the conductor cable. A Hydrostone slurry was mixed in a weight ratio of 45 percent water and 55 percent Hydrostone and filled into a plastic-bag. This was subsequently attached tightly around the end of the steel pipe extending out of the borehole. By squeezing the plastic-bag manually, the contained slurry was delivered through the steel pipe to the bottom of the borehole. While the slurry was enclosing the rock sensor and filling the borehole, the steel pipe was gradually removed. Displacement of air from the hole was accomplished by keeping the bottom end of the pipe in constant contact with the slurry accumulated in the hole. Because of the inclination of the hole axis, e.g., -5 degrees, the slurry was prevented from flowing out before solidification.

4. Installation of Rock-Bolt Sensors.

Prior to installation, a calibration test was conducted on each rock bolt to provide a basis for the strain readings during experimentation (Appendix III). It is interesting to note that the strain values observed were higher than the values computed theoretically. Each bolt was coordinated with a channel of the strain indicator, and the gage bridge was balanced so that a zero strain reading at the indicator was equivalent to a zero strain (and a zero load) on the bolt. The

balance controls of each channel were sealed off by adhesive tape to prevent changes of the correlation base during the period of experimenting.

For each bolt the conductor cable was wound around the bolt shank between the gage position and the carrier plate in the form of 16 to 18 loops, to allow for length compensation during the rotation necessary upon installation. Furthermore, where physically needed, small notches were chiseled into the rock at the borehole edges to allow the cable to slide in and out between the carrier plate and the rock face.

The bolts were anchored by rotation with a manually-operated wrench, at the same time being continuously connected with the static-strain indicator to permit control of the load increase (Plate II). All bolts were loaded to 700 microstrain, which was considered equivalent to a 4000-lb. axial load.

In those cases where bolts had to be removed from the sequence of tests the anchor was left in the borehole. Upon reinstallation it could be used again without difficulty.

5. Configuration of Blastholes and Sensor Units.

The relative positions of the rock bolts, rock-sensors, and shock sources are illustrated in Fig. 8. While the rock bolts (BB-I, BB-II, BB-III, and BB-IV) were kept in their respective positions (H_1, H_2, and H_3) through several sequences of testing, the boreholes for the explosive charges, (BH-I, BH-II, BH-III, and BH-IV), were used alternately. This was done in order to vary the travel distance from the shock source to each individual bolt. A listing of the various testing combinations of charge and sensor positions for the individual blasts is given in Table 2. In addition, the rock-sensors A, B, and C used by

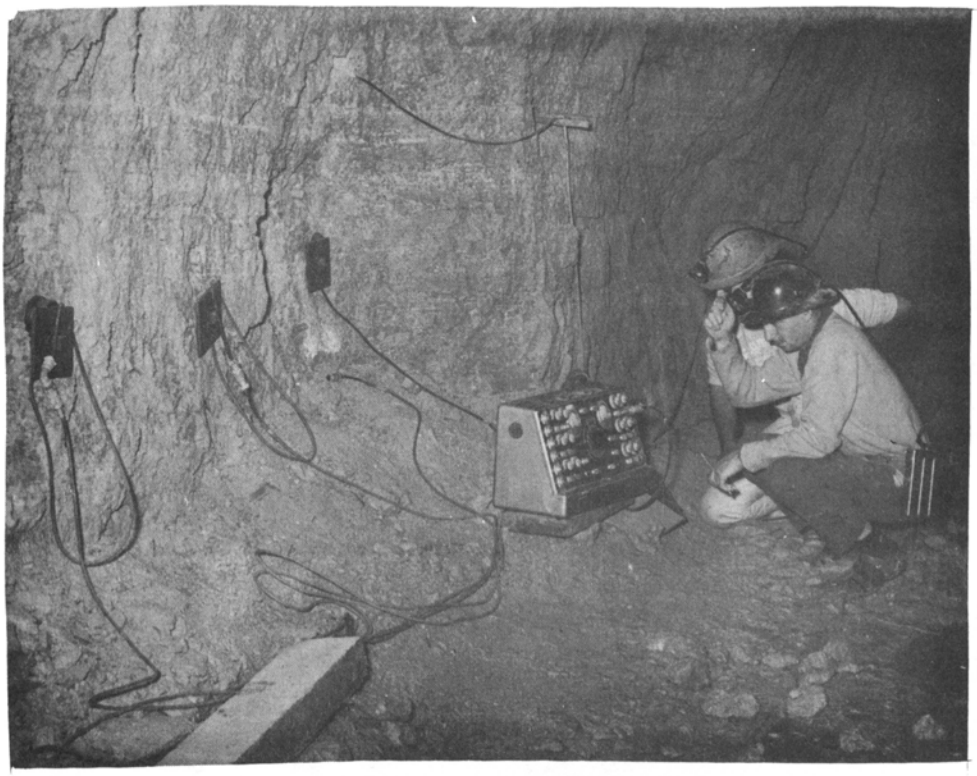

PLATE II

Static Strain Reading at the Test Site.

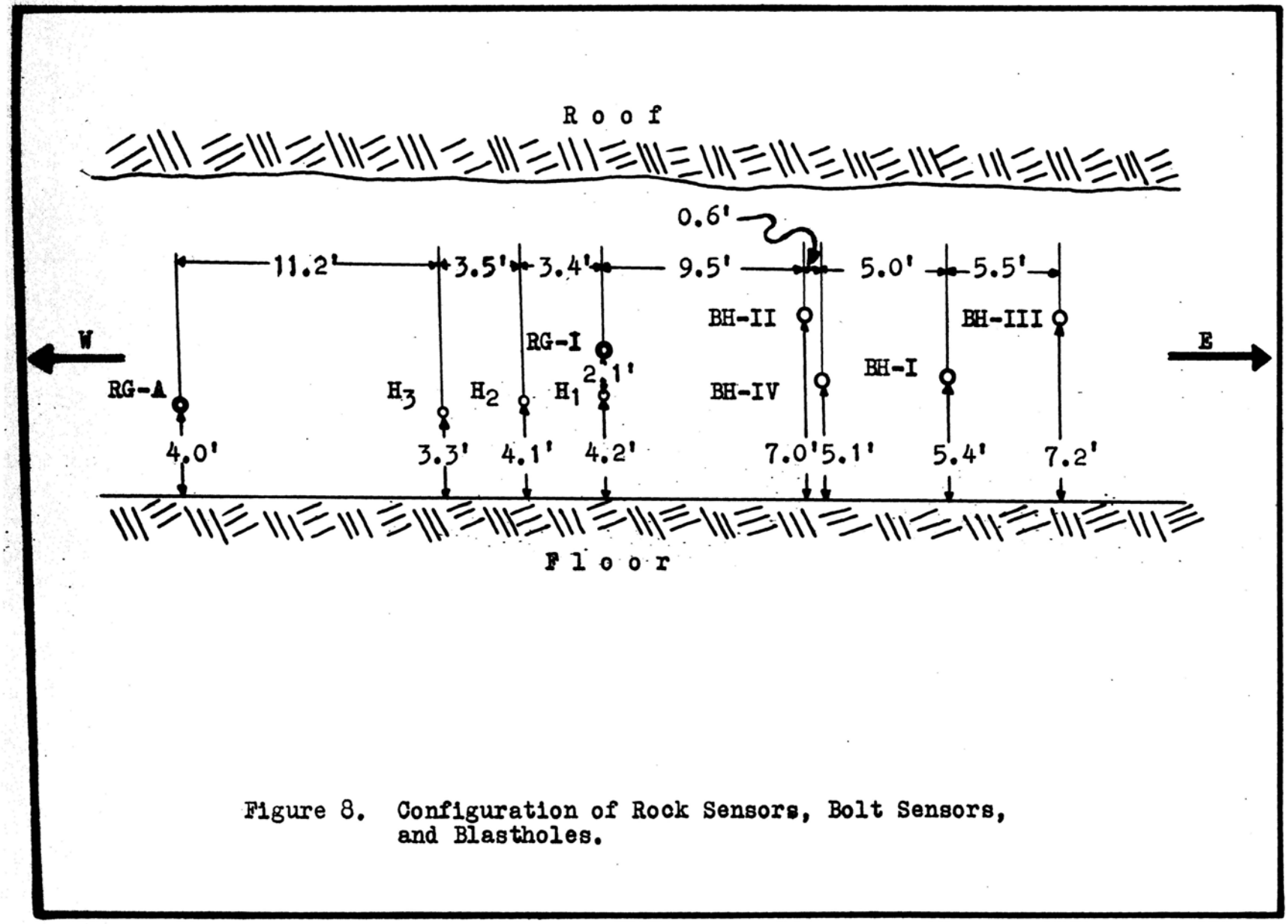

Figure 8. Configuration of Rock Sensors, Bolt Sensors, and Blastholes.

Table 2.

Survey of Test Combinations Between Bolt Sensors,

Rock Sensors, and Blastholes.

Shot Nr.	Rock Sensors Observed		Position of Bolt-Sensors			Shotholes used			
			H_1	H_2	H_3	BH-I	BH-II	BH-III	BH-IV
			Designation of Bolt-Sensor Observed						
1		RG-I			BB-I		BH-II		
2		RG-I			BB-I		BH-II		
3		RG-I			BB-I			BH-III	
4	RG-A	RG-I	BB-IV	BB-II	BB-I			BH-III	
5	RG-A	RG-I	BB-IV	BB-II	BB-I			BH-III	
6	RG-A	RG-I	BB-IV	BB-II	BB-I			BH-III	
7	RG-A	RG-I	BB-IV	BB-II	BB-I			BH-III	
8	RG-A	RG-I	BB-IV	BB-II	BB-I			BH-III	
9	RG-A	RG-I	BB-IV	BB-II	BB-I			BH-III	
10	RG-A	RG-I	BB-IV	BB-II		BH-I			
11	RG-A	RG-I	BB-IV	BB-II				BH-III	
12	RG-A	RG-I	BB-IV	BB-II		BH-I			
13	RG-A	RG-I	BB-IV	BB-II			BH-II		
14	RG-A	RG-I	BB-IV	BB-II	BB-III			BH-III	
15	RG-A	RG-I	BB-IV	BB-II	BB-III	BH-I		BH-III	
16	RG-A	RG-I	BB-IV	BB-II	BB-III	BH-I	BH-II	BH-III	
17	RG-A	RG-I	BB-IV	BB-II	BB-III	BH-I	BH-II	BH-III	
18	RG-A	RG-I	BB-IV	BB-II	BB-III		BH-II		
19	RG-A	RG-I	BB-IV	BB-II	BB-III		BH-II	BH-III	
20	RG-A	RG-I	BB-IV	BB-II	BB-III		BH-II	BH-III	
21	RG-A	RG-I	BB-IV	BB-II	BB-III		BH-II	BH-III	
22	RG-A	RG-I	BB-IV	BB-II	BB-III		BH-II		
23	RG-A	RG-I	BB-IV	BB-II	BB-III		BH-II		
24	RG-A	RG-I	BB-IV	BB-II	BB-III		BH-II		
25	RG-A	RG-I	BB-IV	BB-II	BB-III		BH-II		
26	RG-A	RG-I	BB-IV	BB-II	BB-III	BH-I			
27	RG-A	RG-I	BB-IV	BB-II	BB-III			BH-III	
28	RG-A	RG-I	BB-IV	BB-II	BB-III	BH-I		BH-III	
29	RG-A	RG-I	BB-IV	BB-II	BB-III				BH-IV
30	RG-A	RG-I	BB-IV	BB-II	BB-III		BH-II		BH-IV

Quan in previous experiments (21) are shown.

6. Data Recovery.

As the instrumentation system was designed, two devices for reading strain-data were available: a strain indicator for static conditions and the oscilloscope-camera arrangements for the vibrational phenomena. Thus, very close observation of the sensors was possible by reading the static strain on the rock bolts when installed, just before each blast, immediately thereafter, before dismounting, and after complete removal to check for residual strains. During each blast, the responses from both the rock and bolt-sensors on the oscilloscope screens were photographed. Time of exposure, scale illumination, and intensity of the oscilloscope traces were adjusted by trial in order to produce useful photographs.

Oscilloscopes were turned on before each test series and checked. To avoid time delays due to warm-up and special adjustments as may be required, oscilloscope power remained on throughout each test series. After installation of bolts to the desired amount of strain, the test procedure sequence included the following steps:

a. Record temperature, time, and strain on each bolt immediately before a blasting event, and then reconnect all sensors with the oscilloscope circuitry through the coordinated cables.

b. Tape trigger-sling to explosive primer-cartridge, insert blasting cap, and then load charge into blasthole, with subsequent connection of trigger cable to the sling and blasting cable to the blasting-cap leg-wires. Remove strain indicator from the area.

c. Turn on power to transducer system, preamplifiers, and trigger circuit. Check functioning of oscilloscopes (trace-sensitiv-

ity, sweep, trigger action, amperage of transducer circuit, etc.).

d. Charge blasting condensor and open all camera shutters. Initiate explosive charge by closing blasting-circuit, and promptly close camera shutters after blast. Record time and attitude of oscilloscopes.

e. Shut off power to trigger circuit, preamplifiers, and transducers. Remove exposed photographs from cameras after allowing 15 seconds for complete development.

f. Connect strain-indicator channels to proper bolt sensors and record static-strain readings and time.

DATA INTERPRETATION AND RESULTS

A. Nature of Recovered Data.

A total of 48 test shots was performed for this investigation. No useful data were produced from the first 18 shots, because the recording equipment had to be adjusted and an unsuccessful bolt-sensor design was employed (see Appendix II). Of the remaining 30 test shots, 8 comprised multiple arrangements utilizing standard charges distributed in 2 to 3 blastholes (see Table 2). The purpose of using multiple charges was to observe whether a different pattern in sensor response would result from several simultaneously released shots. No useful data became readily apparent and thus, records of those shots were omitted from interpretation. The remaining 22 shots, which used single standard charges, were made in the sequence and the configurations as listed in Table 2. Data from the latter tests provided the basic source of experimental information.

Static strain measurements yielded direct numerical values. The readings ranged from 700 microstrain (4000-lb. setting load) to 439 microstrain (at the end of the last test-shot series and equivalent to a 2500-lb. load). The dynamic observations were recorded in the form of 66 photographs, yielding a total of 90 usable oscillograph traces (Plate III). Each trace had to be interpreted for its strain indication. This was accomplished first by measuring the recorded peak amplitude of the compressive-strain deflections in centimeters (see Fig. 9). By use of the recorded operating data of the transducing equipment (Appendix V) each amplitude value was then converted into terms of microstrains (Appendix VI). Interpreted traces included 19 from Rock-

Sensor RG-I, 17 from Rock-Sensor A installed by C. K. Quan, and 54 from the various bolt-sensors. There was a large scatter of data in certain cases, probably due to interference between shock waves in the rock medium.

The positions of sensors and blastholes were located by use of a surveying tape to an accuracy of ± 0.1 ft. Time was read from a wrist watch at the instant of each event, exact to full minutes.

B. Interpretation and Discussion of Results.

Static strain readings are compiled in Appendix IV, together with their recorded times of observation and the instants at which blasts were made. The particular blastholes charged and the photographs obtained from each event also are included.

The readings of the peak amplitude from each of the photographed traces are listed in Appendix VI for the rock sensors and the bolt-sensors, along with the identifying numbers of the pertinent blasts. The numerical values for the strain deflections were determined from the traces by use of the operating data shown in Appendix V.

For the interpretation of data, the following points were considered:

a. The consistency of response from tests performed under equal conditions,

b. The trend of the strain loss in bolts for the total experiment and for single tests,

c. The influence of absolute bolt strain on the strain loss,

d. The influence of wave travel distance and of its intensity on the strain loss,

e. The relationship between vibrational responses of the rock and the bolts, and

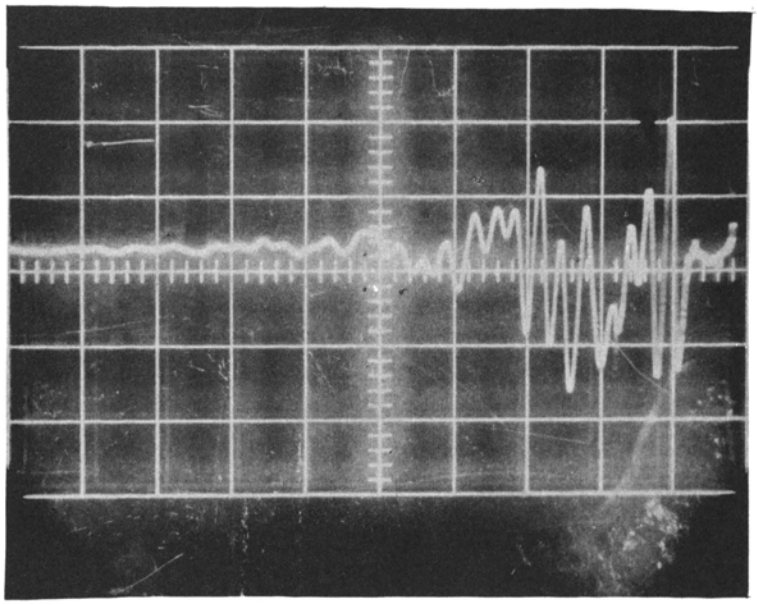

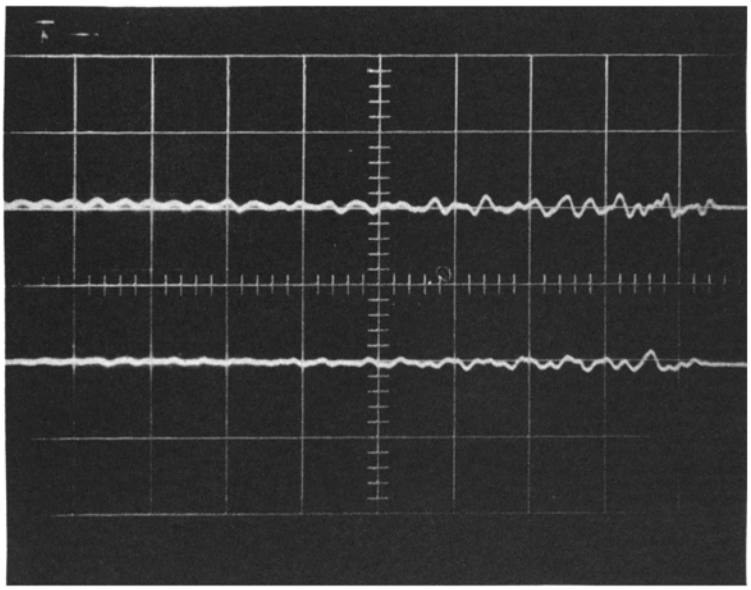

PLATE III

Sample Traces of Rock-Sensor Vibration (above) and Bolt-Sensor Vibration (below) Taken from Shot No. 12.

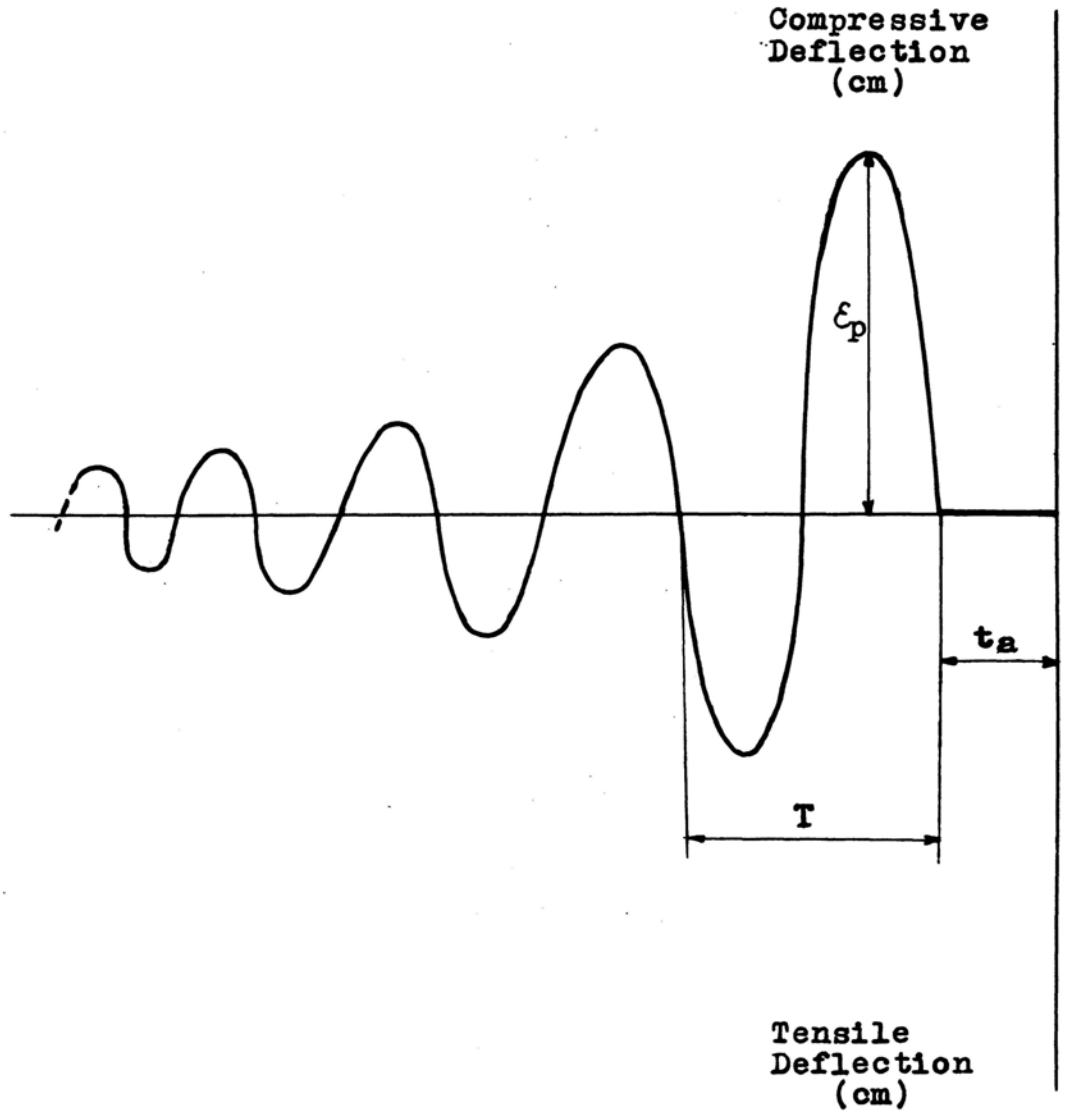

ε_p . . . Peak Strain-Amplitude

t_a . . . Arrival Time

T . . . Vibrational Period

Figure 9. Schematic Oscilloscope Trace.

f. The relationship between vibrational energy and the strain loss in bolts.

1. The Consistency of Sensor Response Under Equal Testing Conditions.

The "equal conditions", mentioned here as a reference for comparison of sensor responses, must be understood as a term with restricted meaning. This is because actual testing conditions could be kept constant only with respect to the geometry of the sensor and blasthole positions and the size of the explosive charge employed.

The entire experimental investigation extended over a period of 32 days. Test shots could be made only when operations in the mine and the investigator's occupation would allow it, so that an adjustment of the testing schedule to favorable conditions was impeded.

Testing conditions with inconsistent character included the natural creep of the anchor during static loading conditions, which effected a continuous decrease of bolt load, and strain losses from the vibrational influences during blasting. Although it would have been possible to reset each bolt to the original setting-load after each test shot, it was preferred to allow the bolts to react freely during the complete experiment in order to closely approach practical conditions.

Another variation was introduced by the change of the blasthole size and shape due to repeated blasting, so that confinement and energy transmission decreased with each additional blast. In close conjunction with this, the rock medium effectively suffered changes in wave conductivity. Not only the propagation of single waves but, especially, the interference of several waves with each other were believed of very inconsistant nature, so that a large scatter of data was created.

Also, variations in moisture present in the mine rock could not be controlled because of the shallow mine openings and the long period of observation.

Because of the influences resulting from changing environmental conditions, it was essential to inspect each data group derived from approximately equal test conditions, for agreement between values, so that possible relationships between different groups might be determined.

2. Strain-Time Relationships.

A graph of strain-time development is given in Fig. 10 for each of the bolts employed. The plots indicate the significant influence of vibrations. It presents the static strain readings taken before each test series and after its completion (see Appendix IV). Readings taken between the subsequent blasts of a series are omitted. Only the quantity of blasts performed in each of the series are indicated on the graph. Since the plots had been established neglecting variations in blasthole positions their validity must be restricted to a range of travel distances varying within an accuracy of $\pm$ 6 ft. for each of the bolts considered. A discussion of the influence of distance on the strain decay will follow in a later section.

The observation times of the bolts were resolved into two parts: the intervals during which they were exposed to vibrations, and the intervals of constant load conditions. Summing up the strain losses of a bolt during all of the observed vibrational part-times and dividing by the cumulative sum of recorded part-times within which the vibrations occurred, a ratio of strain loss per unit time was obtained. The ratio represented the over-all decay gradient of the actual bolt strain during dynamic tests. An equivalent ratio was also set up for the periods of

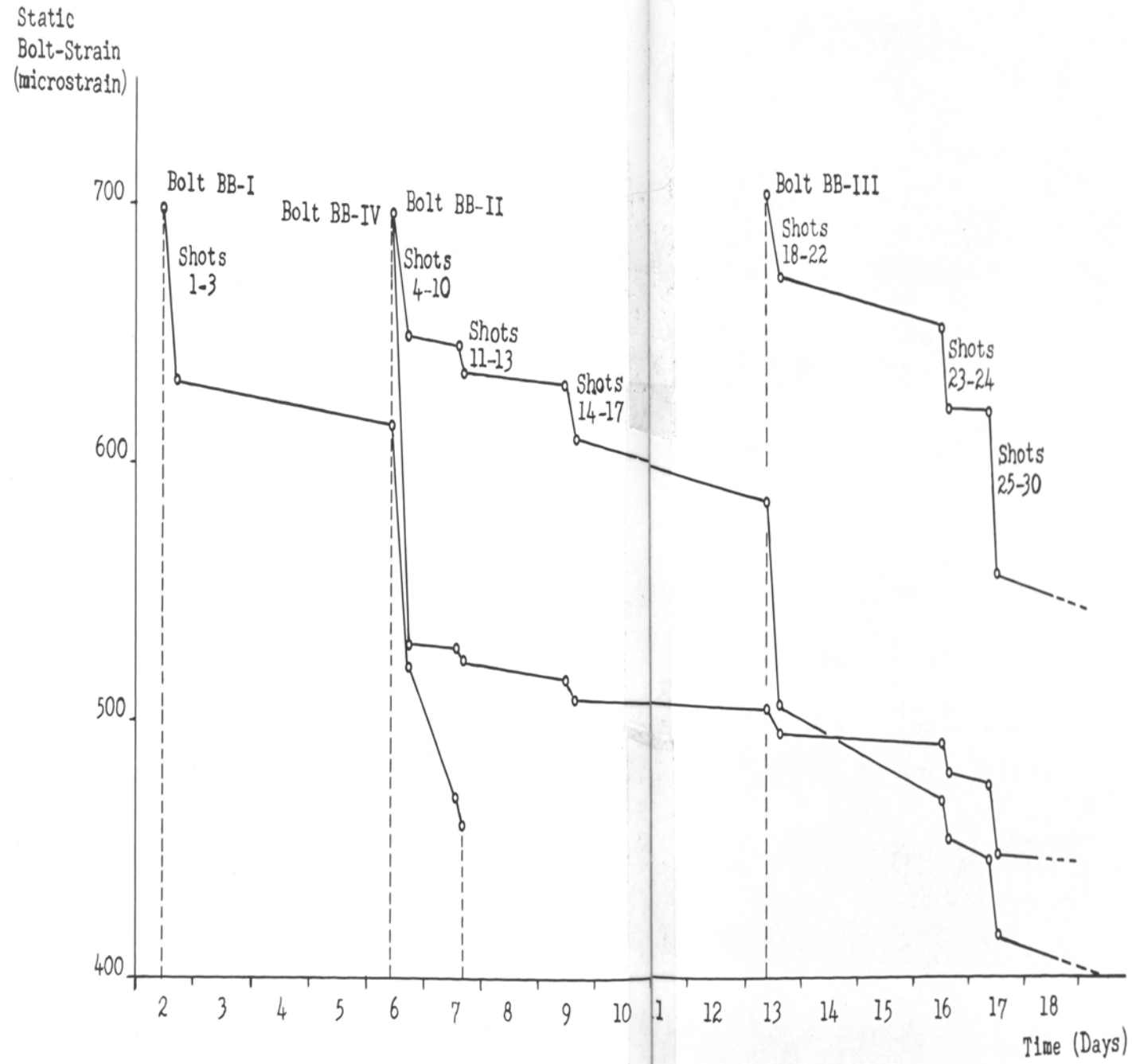

Figure 10. Strain Variation in Bolt Sensors Over the Experiment.

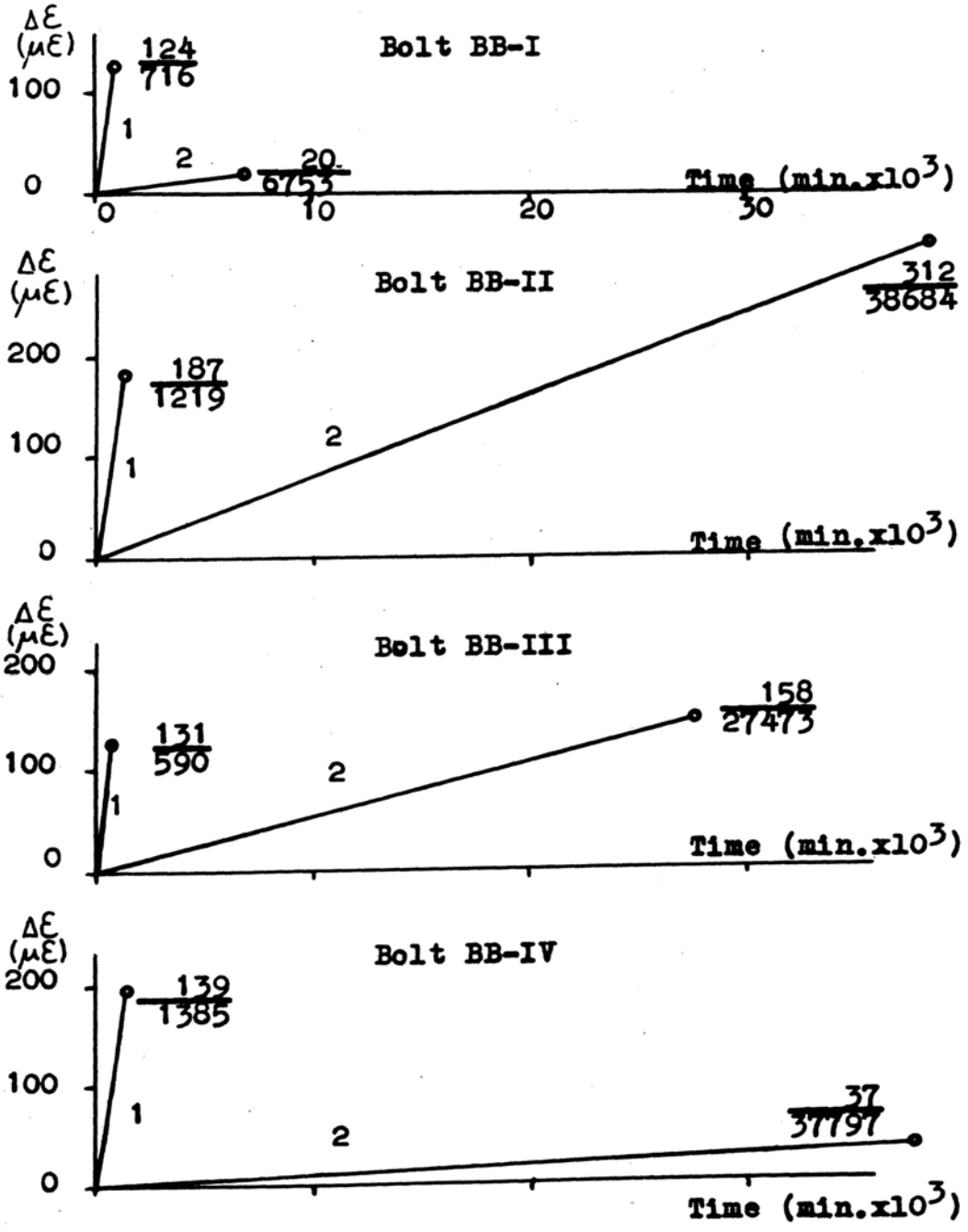

Figure 11. Illustration of Decay Gradients for Vibrational Conditions (Curves 1) and Constant Load Conditions (Curves 2).

static load conditions. Numerically, the decay rates were equal to the following values:

a. Vibrational Periods: 0.10 to 0.20 microstrain/minute, or an average of 0.16 microstrain/minute, for 4 bolts exposed to 30 test-shots.

b. Constant Load Periods: 0.98×10^{-3} to 8.22×10^{-3} microstrain/minute, or an average of 4.48×10^{-3} microstrain/minute, for 4 bolts.

c. Ratio of Average Decay Rates (average from a. divided by average from b.): $0.16/0.00448 = 36$.

The decay rates for the individual bolts are shown in Fig. 11.

Although data for the graphs were affected by variations in geometric configuration and conditions of environment, they indicate that a distinct, uniform stability change occurred from static to vibrational loading conditions. With respect to the particular way data were recovered, it can be concluded that actual decay rates for vibrational part-times would have had much higher values than the ones calculated above. This is because the recorded vibrational part-times spanned several minutes before and after each blasting event. Thus, the data exaggerated the events which actually took place within a few seconds or fractions thereof. The true reference times for the decay gradient could not be observed because of the short time intervals covered by the oscilloscope traces. Also, this deficiency in dynamic recording was held responsible for the failure to observe actual strain loss from the oscilloscope traces.

3. Strain Loss and State of Strain in Bolts.

From the collected data, the extreme values with respect to the amount of strain loss per event were selected to determine the range of influence. The maximum strain loss encountered was 100 microstrain at

Table 3.

Computation of Percent Strain-Loss for the Bolt Sensors.

Bolt-Location	Shot No.	Initial Strain	Strain-Loss	Strain-Loss in Percent	Initial Strain	Strain Loss	Strain-Loss in Percent	Initial Strain	Strain-Loss	Strain-Loss in Percent
		Bolt BB-I			Bolt BB-II			Bolt BB-IV		
BH-II	1	674	16	2.38						
BH-II	2	658	13	1.98						
BH-II	13	465	5	1.08	640	3	0.47	525	2	0.38
		average:		1.81						
		Bolt BB-III								
BH-II	18	708	3	0.42	587	10	1.70			
BH-II	22	687	12	1.75	516	10	1.94			
BH-II	23	657	15	2.28	470	9	2.13	492	7	1.42
BH-II	24	642	18	2.80	461	7	1.52	485	5	1.03
BH-II	25	623	14	2.25	448	5	1.12	476	2	0.42
		average:		1.90	average:		1.48	average:		0.81
		Bolt BB-I			Bolt BB-II			Bolt BB-IV		
BH-I	10	525	4	0.76	651	1	0.15			
BH-I	12	470	5	1.06	642	2	0.32	526	1	0.19
		average:		0.91						
		Bolt BB-III								
BH-I	26	609	6	0.99	443	4	0.90	474	4	0.84
		average:		0.99	average:		0.45	average:		0.52
		Bolt BB-I			Bolt BB-II			Bolt BB-IV		
BH-III	3	645	14	2.17						
BH-III	4	612	36	5.88	684	12	1.76	667	15	2.25
BH-III	5	570	10	1.75	669	4	0.60	645	4	0.62
BH-III	6	560	9	1.61	665	6	0.90	641	1	0.16
BH-III	7	551	6	1.09	659	2	0.29	640	5	0.78
BH-III	8	545	18	3.30	657	4	0.61	635	2	0.32
BH-III	9	527	2	0.38	653	2	0.31	633	3	0.47
		average:		2.31						
		Bolt BB-III								
BH-III	11				647	3	0.46	528	2	0.38
BH-III	14	693	9	1.30	629	5	0.80			
BH-III	27	603	4	0.66	439	4	0.91	470	9	1.91
		average:		0.98	average:		0.74	average:		0.86

an initial bolt strain of 630 microstrain (3,600 lb. load), which in percent of bolt strain was 15.87 percent. The minimum strain loss encountered was 0 microstrain, which occurred at initial bolt strains of 517, 505, 496, and 470 microstrain (2,900, 2,830, 2,770, and 2,620 lb. loads, respectively).

In no case was complete anchorage failure observed during the experiment. In two cases an increase of strain of 4 and 1 microstrain occurred at bolt strains of 515 and 705 microstrain, respectively.

The behavior of the bolts, as shown in Fig. 10, indicated that a change of the decay rate with time occurred. The strain tended to decrease as time increased. Because of the inexact role of time as a quantity for correlation, the state of strain appeared as the more appropriate basis for derivation of a relationship. Therefore, the strain loss was expressed as a percent of the state of strain at the start of each event. Initially, a plot was drawn for each bolt to inspect the data output from shots made at equal distances. The data points showed such an irregular scatter that no relationship could be detected. Therefore the plots were excluded from this thesis.

In order to find the region of strain loss occurring most frequently, a frequency distribution curve was established for the overall experiment, which indicated strain losses in the range from 0.25 percent to 0.50 percent as being the most frequent (Fig 12). It shows that there was only one shot which had a strain loss over 3 percent. The graph was drawn using data from all events for bolt sensors without distinguishing between different travel distances or bolt strains. It is valid, therefore, only for the total range of test configurations used.

Table 4.

Tabulation of Frequency for Classes of Percent Strain-Loss.

Class (%)	Number of Cases	Percent of Cases (%)
0.00	4	7.14
0.001-0.25	3	5.36
0.25 -0.50	12	21.43
0.50 -0.75	4	7.14
0.75 -1.00	8	14.28
1.00 -1.25	5	8.93
1.25 -1.50	2	3.57
1.50 -1.75	4	7.14
1.75 -2.00	5	8.93
2.00 -2.25	4	7.14
2.25 -2.50	2	3.57
2.50 -2.75	0	0.00
2.75 -3.00	1	1.79
3.00 -3.25	0	0.00
3.25 -3.50	1	1.79
3.50 -3.75	0	0.00
3.75 -4.00	0	0.00
4.75 -5.00	1	1.79
Total	56	100.00

Table 5.

Strain-Loss Values from Table 3 Rearranged for Plotting in Fig. 13.

Distance from Shot (ft.)	Average Strain-Loss (%)	Number of Shots Counted	Blasthole	Bolt-Sensor
10.2	1.81	3	BH-II	BB-I
10.2	1.90	5	BH-II	BB-III
13.2	1.48	6	BH-II	BB-II
14.0	0.91	2	BH-I	BB-I
14.0	0.99	1	BH-I	BB-III
16.6	0.81	4	BH-II	BB-IV
19.3	0.45	3	BH-I	BB-II
21.8	2.31	7	BH-III	BB-I
21.8	0.98	2	BH-III	BB-III
22.4	0.52	2	BH-I	BB-IV
24.2	0.74	9	BH-III	BB-II
27.8	0.86	8	BH-III	BB-IV

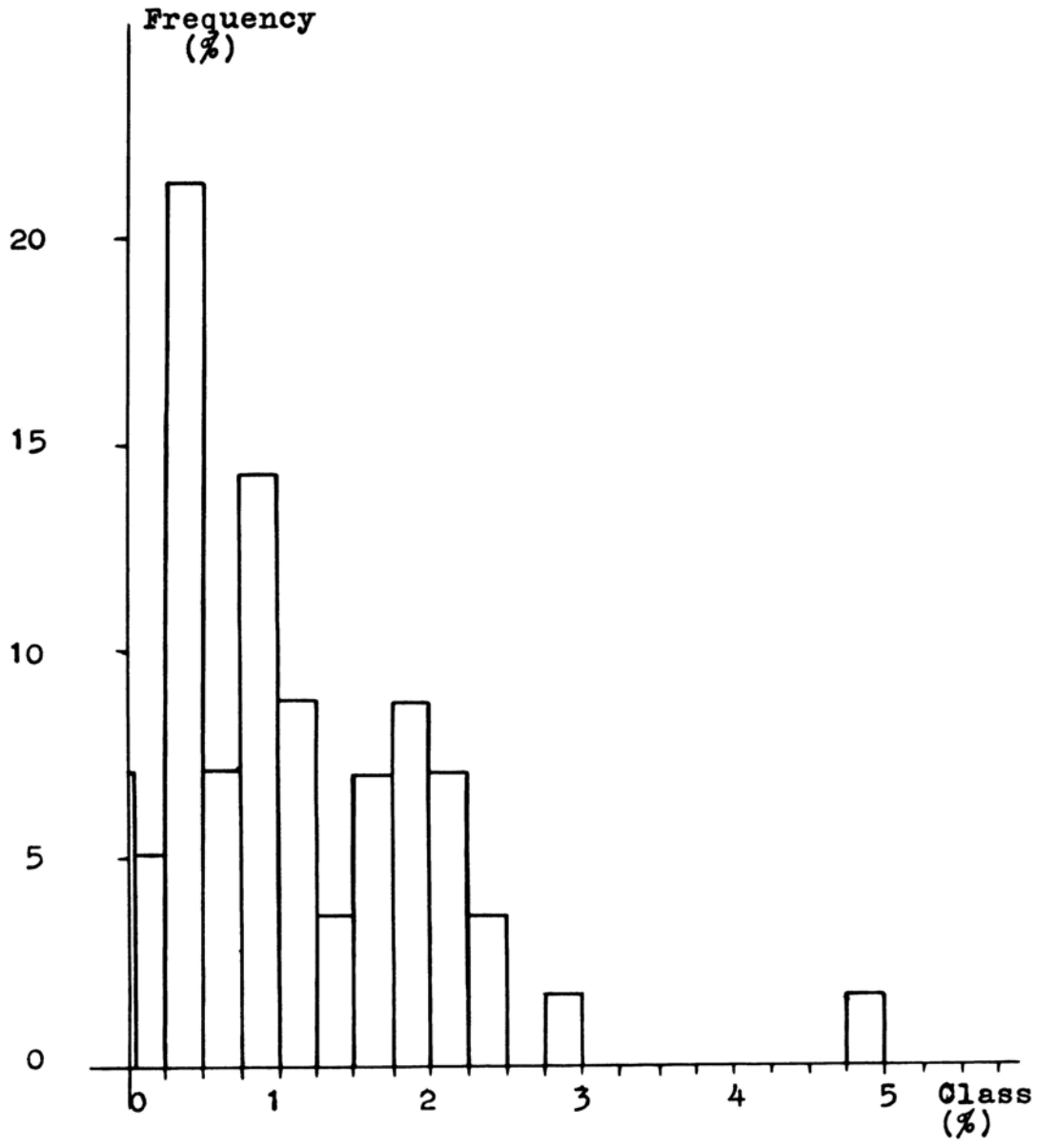

Figure 12. Frequency Distribution of Strain-Losses in Percent.

4. Strain-Loss Distance Relationships.

To show the influence of geometric configuration the data have been separated into groups of constant configuration. As a measure of constant configuration the travel distance from the shock source to the bolt position has been used. From the average values of the data groups, a graph was plotted where the relationship between strain-loss and travel distance was shown (Fig. 13). It was noticed that a much greater increase of strain loss occurred for shock sources within 15 ft. from a bolt position.

5. Comparison of Strain Loss and Vibrational Behavior

Scanning the data in Table 3, a rather high scatter of values was evident. The reason for this might well be due to changes of coupling conditions for the explosive, because of alterations in rock conditions around the blastholes or in interference phenomena between vibrations. To better show the trend of the data, a rearrangement had been made. As an expression of the response intensity of bolts two different quantities were chosen: the vibrational peak strain and the strain loss in percent. Plots were made with respect to the travel distance in Fig. 14 and Fig. 15 (see data in Appendix). In addition, a graph was plotted containing the vibrational peak strains observed from the rock-sensors (Fig. 16). In all three figures the data points are designated by the shot number to which they belong. Thus, a comparison was possible between the effects of any test shot on several sensors.

The data distribution in Fig. 14 and Fig. 15 at a travel distance of 17 ft. suggests there was a minimum influence on recorded peak amplitudes and strain losses of bolts. For both increasing and decreasing travel distances, the peak strain-amplitudes of bolts increased and

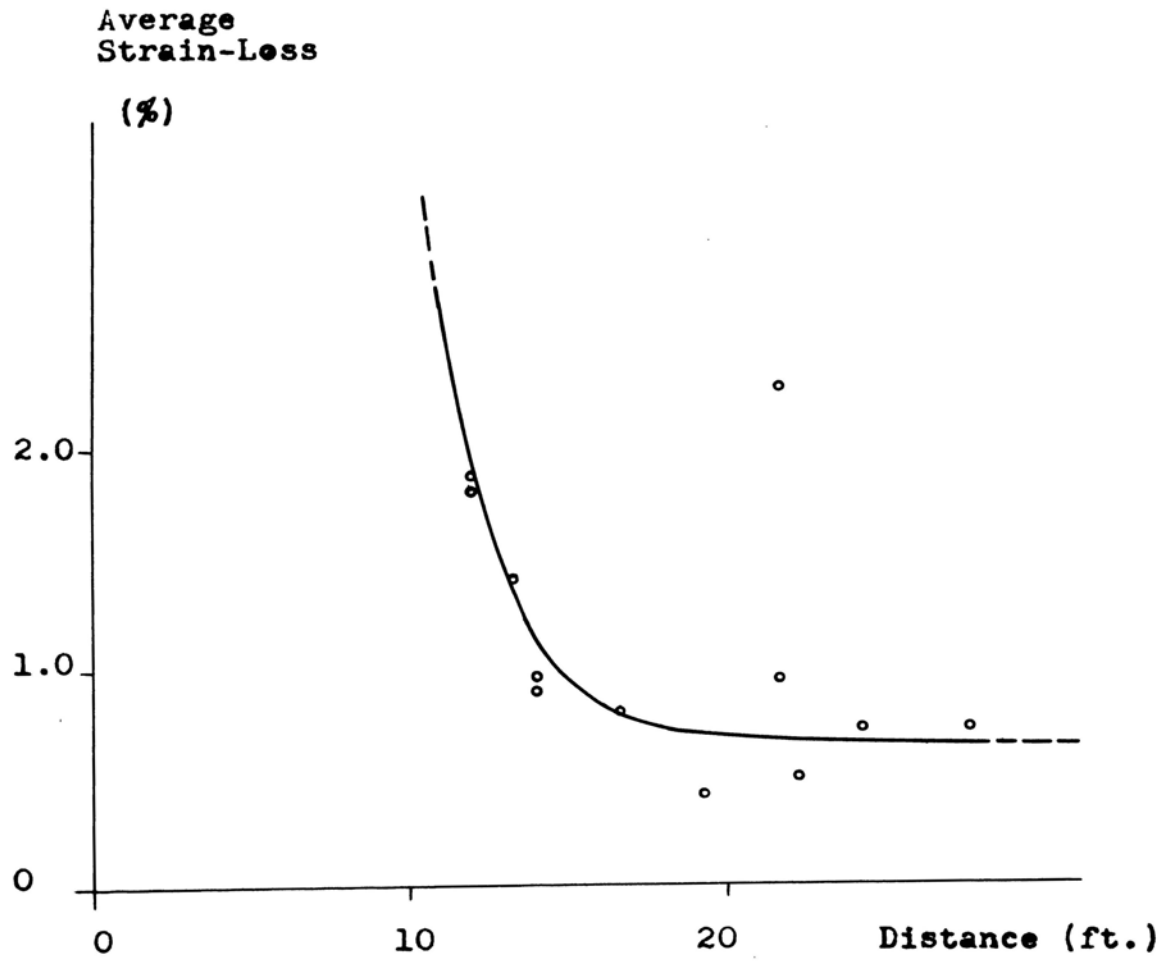

Figure 13. Relationship Between Average Strain-Loss in Percent and Travel Distance.

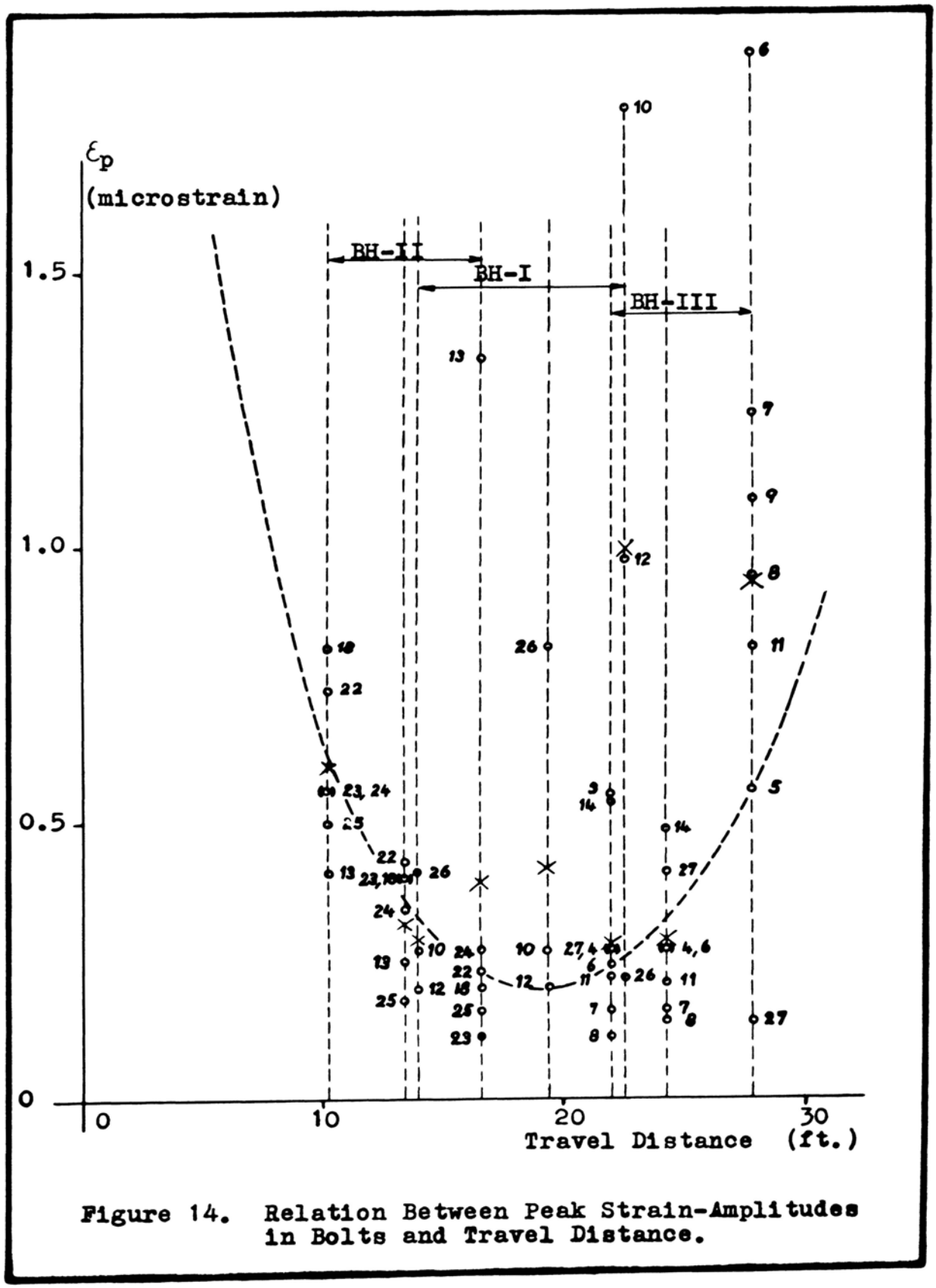

Figure 14. Relation Between Peak Strain-Amplitudes in Bolts and Travel Distance.

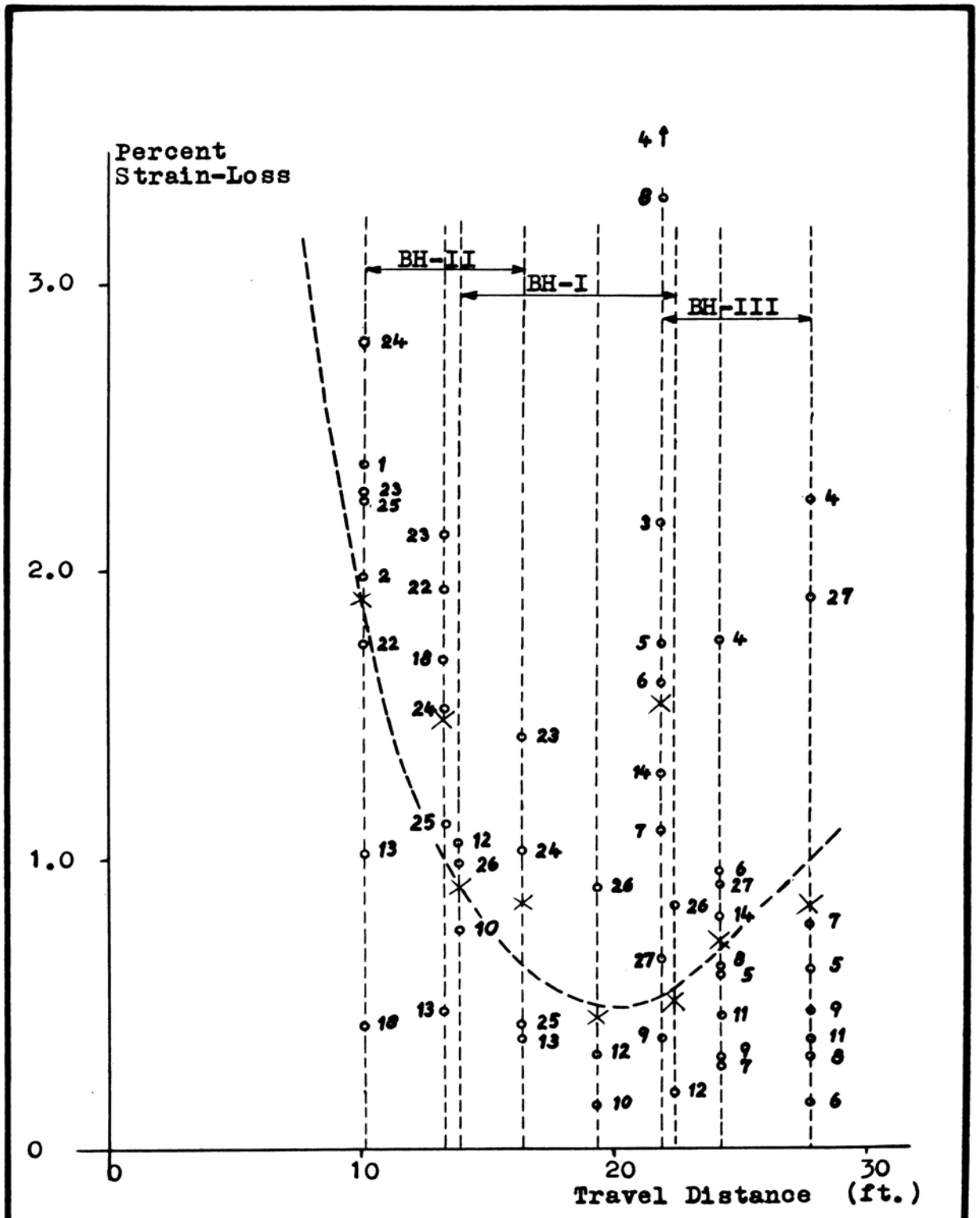

Figure 15. Relationship Between Percent Strain-Loss in Bolts and Travel Distance.

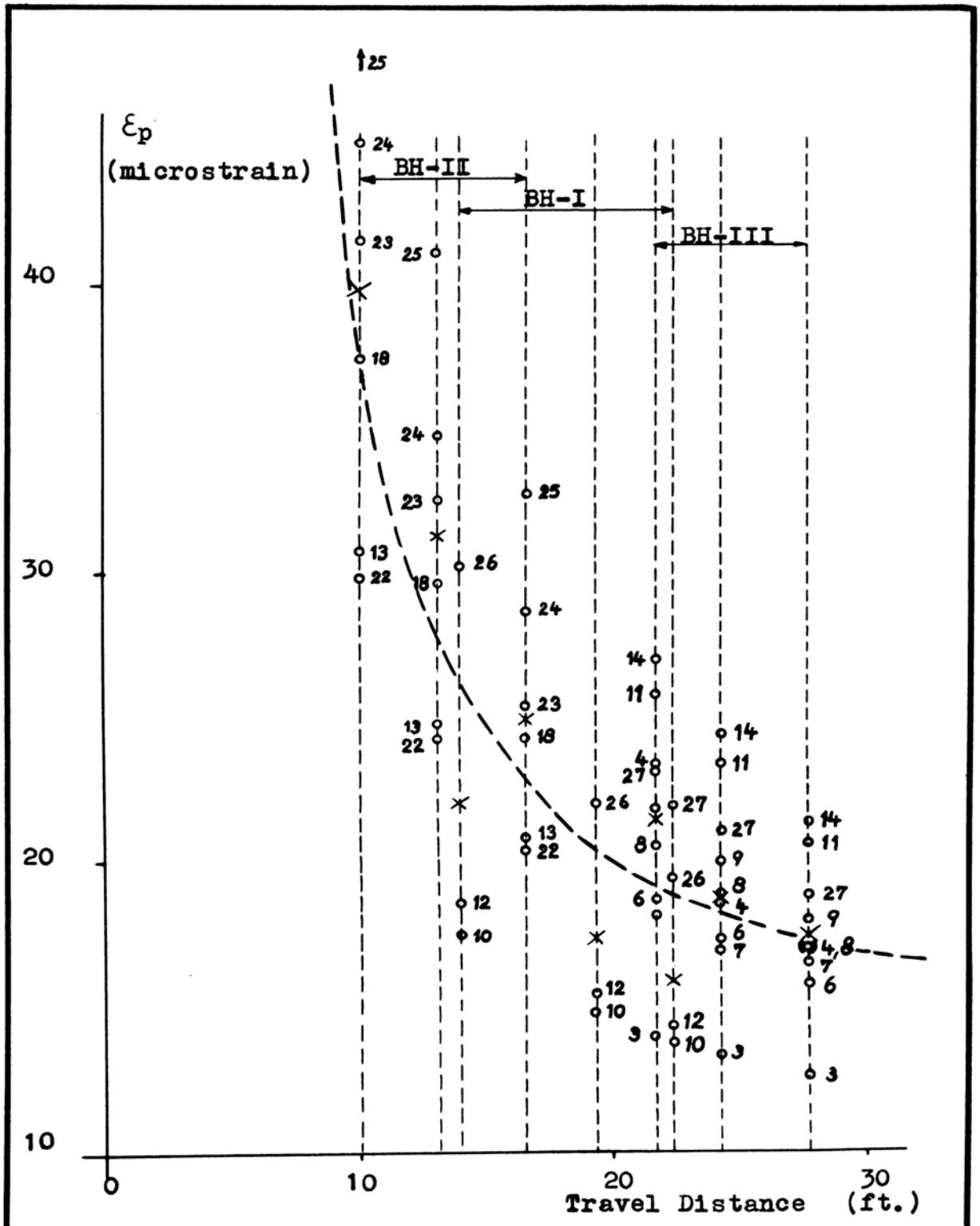

Figure 16. Relationship Between Peak Strain-Amplitudes in Rock and Travel Distance.

scatter of data points became greater. As is obvious from Fig. 16, the effects did not occur for the rock sensors. It would appear then, that the rock vibrations did not reflect the effects on the strain loss as distinctly as did the bolt vibrations.

The peak amplitudes of rock vibrations were at high multiples of those for bolt vibrations. The divergence of the responses indicated incomplete transmission of the vibrations from rock to bolts, possibly because of partial rock failure or relative movement at the contact points. Since yielding at the carrier plates was improbable, and unscrewing of the bolts was not observed, losses in bolt strain must be attributed to displacements of the anchors.

6. Relationships Between Vibrational Energy and Anchorage Stability.

The strain loss of a tensioned bolt is a transition from a higher potential state to a lower one. To contribute further to an understanding of the anchorage failure, the phenomenon of strain loss was investigated with respect to certain energy quantities. Based on the nature of this experiment, values for both the energy of bolt vibration and rock-vibration were derived from the oscilloscope traces. From the peak strain-amplitudes (Appendix VI), the peak energies of vibration were calculated for each event. For computation the following formula was used, which was derived from laws of elastic vibration (24, 25, 26):

$$E = \mathcal{E}_p^{\,2}\, S/2, \qquad 6.$$

where E is the vibrational energy, $\mathcal{E}_p$ is the peak strain-amplitude, and S is the so-called Spring Stiffness. The formula was applied for determining the vibrational energy transmitted through a unit volume of the medium at any particular instant of time. For calculations, the unit

volume of a cylinder with a 3/4-in. diameter and a 1-in. length was selected as a constant reference. This shape and size was chosen to conform with the dimensions of the bolts used. The values of the Spring Stiffness were computed for this body from the elastic properties of steel and rock under the assumption of ideal elastic behavior. The exact procedure for the numerical evaluation is shown in Appendix VII and VIII. As a first step, the energy of rock vibration was determined for the positions of the bolt sensors by use of the extrapolated strain data (Appendix VII).

The vibrational energies of the bolt sensors were found directly from the peak strains determined from the pertinent oscilloscope traces. They are listed in Appendix VIII. Both groups of data did not allow recognition of significant features by simple inspection. For correlation, an empirical curve was established, as shown in Fig 17. The ratio of vibrational energy in the rock divided by the vibrational energy in a bolt was selected to express the degree of energy transmission at the anchor. The ratio was plotted against the corresponding strain-losses in percent. The graph indicated a distinct increase of strain loss with increasing energy ratio, following an exponential relationship. It was interesting to observe that the values of vibratory energy transmitted to the bolts were at fractions of approximately 1/10 to 1/350 of the vibrational energy occuring in the rock. This also represented an indication of the discontinuity of motion at the bolt-to-rock contacts.

Table 6.

Energy Ratios (E_r/E_b) as Determined from Appendix VII and VIII.

Shot No.	Blasthole	Bolt-Sensor Positions		
		H_1	H_2	H_3
3	BH-III	5.57	--	--
4	BH-III	151.00	113.50	--
6	BH-III	140.00	78.80	3.20
7	BH-III	284.00	204.00	20.70
8	BH-III	1150.00*	49.80	5.84
9	BH-III	--	--	5.80
10	BH-I	51.00	33.90	0.49*
11	BH-III	559.00	414.00	17.50
12	BH-I	182.50	73.30	2.05
13	BH-II	284.00	395.00	6.59
14	BH-III	108.10	93.60	--
18	BH-II	128.50	253.00	520.00*
22	BH-II	79.20	119.50	213.00
23	BH-II	349.00	339.00	2600.00*
24	BH-II	425.00	579.00*	515.00*
25	BH-II	823.00	3380.00*	2180.00*
26	BH-I	267.00	24.30*	19.70
27	BH-III	252.00	79.30	420.00

Note: * indicates data omitted from interpretation because of extreme magnitudes.

Table 7.

Average Energy Ratios and Corresponding Average Strain-Losses.

Travel Distance (ft.)	Average Strain-Loss (%)	Energy Ratio Average
10.2	1.76	348.1
13.2	1.55	276.1
14.0	0.94	166.8
16.6	0.95	244.8
19.3	0.44	53.9
21.8	1.89	213.1
22.4	0.52	10.9
24.2	0.74	129.1
27.8	0.50	79.7

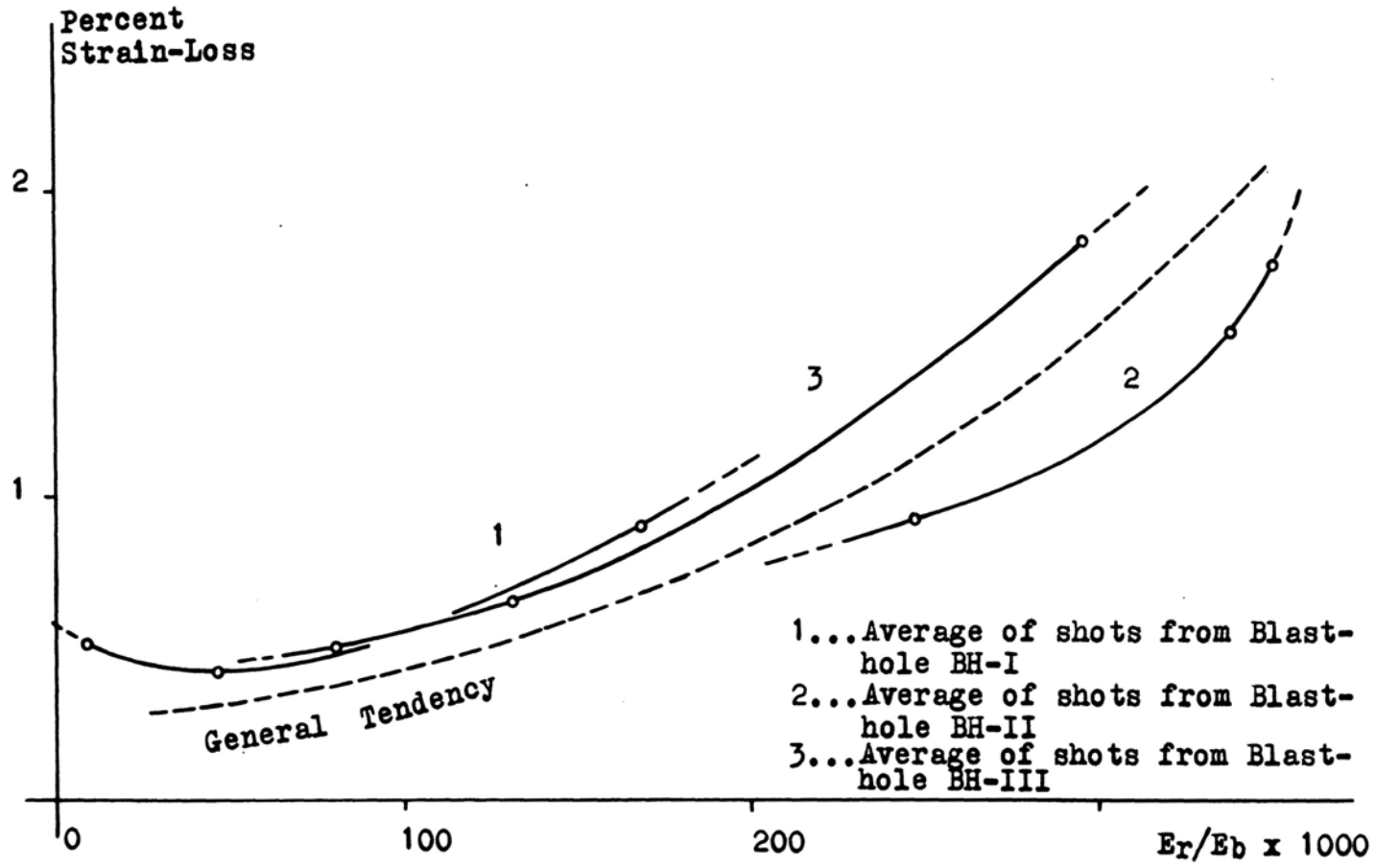

Figure 17. Relationship Between Energy Ratio (E_r/E_b) and Percent Strain-Loss.

CONCLUSIONS AND RECOMMENDATIONS.

A. Conclusions.

Summarizing the results of the entire experiment, the following conclusions can be drawn:

1. A natural decay of the bolt strain occurred during periods of static loading, similar to long-term creep.

2. Shock waves affected the stability of bolts by inducing an abrupt drop in strain and long-term creep continued after blasts.

3. All observed bolts reacted to vibrations with a strain loss.

4. The amount of strain loss varied directly with the intensity of the shock waves but varied inversely with the travel distance of waves.

5. Under the test conditions, percent strain-loss was greatest when the shot distance was less than 15 ft.

6. A complete failure of anchorage under the test conditions did not occur, but yielding at the anchor-to-rock contact was indicated.

7. In the majority of tests the percent strain-loss was less than 1 percent and was rarely over 2 percent.

8. Measurement of bolt vibrations provided a better means to predict anchorage stability than did measurement of rock vibrations.

9. Rock bolts showed little promise for success as a tool to observe dynamic rock behavior.

10. The vibratory energy observed in bolts was only 1/10 to 1/350 of the vibratory energy observed in rock.

B. Practical Significance of the Investigation.

From Stehlik's (27) investigation of rock bolt stability under dynamic conditions performed at the White Pine Mine, White Pine, Michigan, a

decay of stability, and failure in some instances, of bolts was reported. Due to limitations imposed by production requirements, it was not possible to ascertain correlations between losses of anchorage and the vibrations released by blasts. It was thought that the activity of tectonic rock stresses and artificially induced stresses in mine rock might well have contributed to the observed effects, possibly by establishing stress conditions that were close to exceeding anchorage-stability limits. The results from this present study confirmed that there could be detrimental effects from vibrations on bolt stability. Thus, Stehlik's hypothetical explanation for those instances in which yielding occurred without horizontal shifting of the roof strata appears to have considerable merit.

1. Aspects of Large-Scale and Multiple-Charge Blasts.

Although an explosive charge-weight of only 0.9 lb. as used in these studies, was not comparable in size to that commonly employed in most mining operations, the vibrational characteristics of the blast waves would be indicative of those that could be expected from a larger sized charge. In general, shock wave intensities vary as the cube root of the ratio of charge weights. For a charge weight of 8 lb., representing the average explosive charge for an 8 to 10 ft. blasthole, the intensity of the wave generated would be at least double that produced from the 0.9 lb. at an equal travel distance. Increased hole depths and multiple charges fired simultaneously would greatly intensify the effects.

For a series of multiple charges it also could be expected that interference of the several wave trains would result in either cancellation or fortification of vibrations. The same effect could occur at the intersection of wave fronts produced at points of petrographic discontinuities. Thus, certain blast configurations would seriously affect

anchorage stability to the danger point, or for some cases, bolts could remain unaffected within a critical proximity of blasts.

2. The Influence of Overburden Depth and Stress on Sensitivity to Vibrations.

Bolt loads and the state of rock stress in this investigation had been well below those values common to most mine support conditions. Based on theoretical considerations (see Chapter II, Section B. 2), bolt stability would approach a critical state as the acting load increases. Also, most active stresses within a rock body as found at depth will increase a bolt's sensitivity to vibrations. This is because rocks exhibit the general tendency to become more rigid and absorb less shock wave energy as depth increases. Thus, the combination of possibly increased stress conditions, better susceptibility to the propagation of vibrational energy, and the likelihood of tectonic activity at depth could present serious problems in the maintenance of proper bolt anchorage.

3. Effects Due to Bolt Position Relative to the Direction of Wave Propagation.

As the experiment was performed, no variation of the wave propagation direction relative to the axes of the bolts was attempted. In all tests, the bolts were exposed to waves propagated perpendicular to the bolt axis. This is believed to represent most field conditions, since the majority of rock bolting is utilized in stratified rock, where the bolt axis lies perpendicular to the stratification.

It is assumed that a wave travelling parallel to strata planes will cause primary dynamic strains in the direction of stratification. Secondary strains will develop across the strata in accordance with the rock's characteristic Poisson's Ratio. The resulting swell, or

contraction of strata, is believed to act on the bolt in the form of an addition of active stresses. Wave fronts propagated directly parallel with the bolt axis should cause maximum strains to result transverse to the rock stratification. The structural configuration for this form of incidence necessarily would exist when waves are released in mine levels above the bolt site, or at a distance in the direction of stratification where the shock energy is transmitted by multiple reflections at strata interplanes. In most of the latter cases, the wave intensity at the bolt site will be some fraction or multiple of the original intensity, and their influence would be difficult to estimate. According to some of the data (Fig. 15 and Fig. 16) obtained in this investigation, even feeble rock vibrations occasionally initiated large losses in bolt strain.

A high sensitivity to axial straining is indicated from the mechanical principles of anchorage, especially when considering the stress distribution around the contact of individual serrations of the anchor shell (18). This feature suggests that shocks propagated parallel to the bolt axis, despite their greater losses of intensity during propagation, affect bolt stability perhaps more severely than shocks moving perpendicular to the bolt axis.

4. Feasibility of Bolt Retightening.

Generally, it is impossible to eliminate vibrations in mine structures and imprudent to avoid rock bolting in influenced zones. Bolts with expansion-shell type anchors allow simple retightening of the wedge assemblies, so that each original bolt load can be reestablished as long as the rock and bolt remain intact. The systematic performance of such retightening appears feasible to limit damage to bolted mine

structures. Work by Stefanko indicated that retightening of bolts increased their long-term stability.

During events that loosen anchors, a destressing of the rock compound and dislocation of rock sections takes place. It seems improbable that such alterations can be completely corrected by retightening of bolts, because of the limited forces transferable through rock bolts. On the other hand, retightening inhibits continuation of the failure process and increases structural stability in most conditions. It is believed that even better anchorage stability could be reached through the resetting, because an adjustment of the borehole wall to the shape of the shell surface is expected to take place during vibrational periods. This is because a better form fit and a better stress distribution at the contact will be reached on retightening.

C. Recommendations for Further Investigations.

A continuation of studies on rock bolt behavior during dynamic loading is recommended to solidify the gained experience and to further clarify the relationships indicated by this investigation. Future tests should be conducted in a rock which is more homogeneous to reduce the scatter of data. With more favorable rock properties, it is suggested that a rock-sensor be placed in the immediate proximity of a bolt-sensor, so that it comes within the stress field induced by the bolt's clamping action. The rock-sensor, then, can be expected to yield better data for comparison with the bolt response.

From theoretical considerations, it would appear that sensitivity to vibrations should be highest for a configuration on which wave fronts are propagated parallel to the bolt axis. An investigation of this problem could provide valuable data toward improvement of rock bolting practices.

Also, there is a wide field open for investigations on anchorage stability at various levels of bolt setting-loads, blast intensities, travel distances, and at various arrangements of multiple charges and delay times.

A greater demand will be placed on the recording equipment as future testing projects become more complex or more specialized. Even for the type of observation performed, it was found preferable to employ more highly developed equipment than was available. In particular, recorders that function on optic or electromagnetic principles with gradually adjustable recording speeds and recording times allow suitable adjustments for the complete recording of individual events. If equipped with a large number of channels, they could produce a greater data output. Thus, a better comprehension of the nature of shock waves would be possible and a greater number of data for statistical treatment would become available.

Model studies of the character as reported by Hartman and Tandanand (28), which permit continuous observation of dynamic phenomena occurring at the anchor-to-rock contact, would be most beneficial in developing terms of highest informative value and for directing further investigative steps.

APPENDIX I

LIST OF SYMBOLS.

P . . . . Force acting axially along bolt shank (lb.).

L_r . . . . Force acting on carrier plate (lb.).

P_a . . . . Force developed by rock to maintain equilibrium with the force, P, exerted by the bolt (lb.).

τ_a . . . . Axial shear stress acting on leaf-rock interface (psi).

σ_r . . . . Radial normal stress acting on leaf-rock interface (psi).

μ_w . . . . Friction coefficient at wedge-leaf interface (constant).

μ_r . . . . Friction coefficient at leaf-rock interface (constant).

β . . . . Angle of wedge slope (degree).

s . . . . Slope of wedge, equal to $\tan\beta$ (constant).

A . . . . Area of contact between sum of leaves and rock ($in.^2$).

n . . . . Number of leaves.

σ_{r1} . . . . Static normal stress acting on anchor in radial direction (psi).

σ_{r2} . . . . Static normal stress acting on rock in radial direction (psi).

τ_{a1} . . . . Static shear stress acting axially along anchor (psi).

τ_{a2} . . . . Static shear stress acting axially along rock (psi).

σ_i . . . . Vibratory stress incident on shell-to-rock interface (psi).

σ_{v1} . . . . Vibratory normal stress reflected into rock (psi).

τ_{v1} . . . . Vibratory shear stress reflected into rock (psi).

α . . . . Angle of incidence (degree).

σ_{v2} . . . . Vibratory normal stress transmitted into anchor (psi).

τ_{v2} . . . . Vibratory shear stress transmitted into anchor (psi).

APPENDIX I

(Continued)

σ . . . . Normal stress (psi).

ε . . . . Normal strain (microstrain).

ε_p . . . . Peak strain-amplitude (microstrain).

$\Delta\varepsilon$ . . . . Strain difference in absolute values, or in percent.

dE . . . . Voltage difference at transducer output (volt).

R_g . . . . Electrical resistance of strain gage (ohm).

R_s . . . . Electrical input resistance of transducer circuit (ohm).

S_m . . . . Gage Factor for strain gage (constant).

I . . . . Current input to transducer circuit (amp.).

S . . . . Spring Stiffness (lb./microstrain).

S_b . . . . Spring Stiffness of bolt (lb./microstrain).

S_r . . . . Spring Stiffness of rock (lb./microstrain).

a . . . . Area of cross-section of cylindrical reference body ($in.^2$).

E_b . . . . Vibrational energy in bolt (in.-lb. x 10^{-6}).

E_r . . . . Vibrational energy in rock (in.-lb. x 10^{-6}).

K . . . . Constant (see reference 21).

c . . . . Absorption Constant (see reference 21).

r . . . . Distance from shock source to the rock sensor RG-I (ft.).

x . . . . Distance from shock source to bolt sensor (ft.).

e . . . . Base of natural logarithm.

APPENDIX II

DISCUSSION OF DIFFICULTIES ENCOUNTERED DURING EXPERIMENTATION.

A. Difficulties in Construction of Bolt-Sensors.

From indications conveyed in the literature (3), it was assumed that mounting of a single strain gage on each bolt would be sufficient in order to obtain reliable readings. Thus, three rock bolts were initially prepared with one strain gage mounted on each in a position for sensitivity to axial strain. For their mounting, Eastman-910 cement was used, with proper treatment of the gage and the placement area of the bolt prior to attaching the gages. After the recommended drying period, the bolts were tested for proper gage response. A copper-foil was wrapped around the gage position to provide electronic shielding (see Fig. 4). The space between the shield and the bolt shank was then filled with wax having dielectric properties, being poured in at a temperature of 150° F. As was found later, the wax, or the wax at this temperature state, must have interfered with the bonding cement in that proper response of the gages was disturbed. For example, during the use of these bolts at the test site, two of the gages exhibited a continuous drifting effect on the strain indication, when static-strain readings were taken. In spite of this, the bolt sensors showed a prompt response to dynamic strain waves. Therefore, they were employed for the short preliminary testing period, i.e., the initial 18 test-shots, to permit the preliminary adjustments and coordination of recording equipment. When no explanation other than bonding failure could be found during this period, the bolts were dismounted and checked for their stress-strain response. Again, drifting and discontinuities occurred in the strain data observed. On removing the copper-shield and the wax-coating, in order to visually

APPENDIX II

(Continued)

inspect the gage bond, it was observed that the gages had peeled off the shank, together with the wax.

It was decided to substitute an epoxy for the wax, and Du Pont Duco-Cement for the Eastman-910 cement, in the construction of the bolt sensors. Also, the readings from the initial single strain gages had shown some influence from bending moments when the installed bolts were rotated. In order to exclude this disturbance and possible influences from temperature variations, it was felt necessary to find another strain-gage arrangement.

After various considerations a design used by Stefanko (1, 10) was accepted, because it seemed to be the most promising in fulfilling the abovementioned requirements. It also maintained the same electrical resistance and the same gage factor for both static and dynamic testing conditions. Thus, it could be used in the already developed transducing circuits without any alterations. The design was applied as described by Fig. 4 and Fig. 5. No serious inconsistency in its performance had been observed throughout the experiments.

B. Difficulties in Obtaining Data-Records.

Considerable time was spent in eliminating electronic noise which restricted the clarity of oscilloscope traces. The dry-cell batteries were continuously checked, and the automobile-batteries were recharged before each testing series to accomplish this aim. Most of the noise was found to come from the cable connectors that were exposed to the humidity inside the mine. Insulation provided by a wrapping of electrical insulating tape decreased the noise effects considerably, but direct

APPENDIX II

(Continued)

drying of the connectors by use of an electrical hot-air blower was necessary in some cases.

The production of photographs from oscilloscope traces presented problems. For some events the triggering mechanism of the oscilloscopes failed. It was found that a major difficulty was the adjusting for proper screen-illumination and trace-intensity whenever blasthole positions were changed. Due to the design of oscilloscopes, a change in trace-sensitivity had the effect of an automatically opposite change of trace-intensity. Because of this feature, in many cases, the intensities of sections of recorded traces became faint. Another negative influence on the success in photographing was the inconsistency of the quality of the Polaroid films which frequently exhibited a lack of developer gelatin. This had the effect that occasionally parts or all of a photograph remained undeveloped after removal from the camera.

APPENDIX III

A. ROCK-BOLT PROPERTIES.

Bolt:

Bolt Length	60 in.
Shank Diameter	3/4 in.
Yield Point	58,000 psi.
Ultimate Strength	91,000 psi.
Minimum Elongation	13 % in an 8-in. length.
Thread	Rolled thread of 3/4 in. diameter, right hand.
Threaded Length	8.2 in., with 10 threads per inch.
Head	Forged square head with forged neck and flash.

Anchor:

Wedge-and-leaf type, with two leaves on bail, for use in boreholes with a diameter of 1-3/8 in.

Carrier Plate:

Size	6x6x3/8 $in.^3$.

APPENDIX III

B. COMPILATION OF RECORDED DATA FOR CALIBRATION OF BOLT SENSORS.

Bolt BB-I			Bolt BB-II		
Load (lb)	Strain (micro-strain)	Strain (micro-strain)	Load (lb)	Strain (micro-strain)	Strain (micro-strain)
	Loading	Unloading		Loading	Unloading
0	0	0	0	0	-3
200	38	36	200	11	9
400	83	78	400	48	45
600	115	106	600	87	82
800	149	142	800	125	118
1000	183	168	1000	159	154
1200	218	206	1200	200	188
1400	254	240	1400	236	226
1600	291	274	1600	273	263
1800	324	311	1800	309	299
2000	360	347	2000	346	335
2200	398	382	2200	389	372
2400	435	416	2400	420	407
2600	465	452	2600	461	444
2800	500	487	2800	493	480
3000	536	522	3000	532	517
3200	572	559	3200	572	555
3400	606	598	3400	604	592
3600	644	632	3600	640	626
3800	679	665	3800	677	666
4000	714	700	4000	716	701
4200	746	738	4200	751	740
4400	783	780	4400	792	777
4600	818	810	4600	826	814
4800	850	845	4800	862	851
5000	885	885	5000	898	898

APPENDIX III

(B. Continued)

Bolt BB-III			Bolt BB-IV		
Load (lb)	Strain (micro-strain)	Strain (micro-strain)	Load (lb)	Strain (micro-strain)	Strain (micro-strain)
	Loading	Unloading		Loading	Unloading
0	0	-1	0	0	2
200	31	29	200	44	40
400	66	64	400	81	75
600	100	99	600	116	111
800	134	132	800	150	145
1000	172	168	1000	187	180
1200	207	203	1200	222	217
1400	242	237	1400	258	251
1600	278	272	1600	292	286
1800	313	308	1800	331	320
2000	351	343	2000	367	357
2200	386	380	2200	403	391
2400	421	412	2400	439	426
2600	457	449	2600	475	462
2800	496	483	2800	511	498
3000	529	519	3000	546	532
3200	564	555	3200	580	567
3400	600	590	3400	614	603
3600	636	627	3600	650	640
3800	671	663	3800	688	675
4000	708	699	4000	721	709
4200	742	733	4200	757	744
4400	777	768	4400	793	780
4600	816	806	4600	824	817
4800	850	841	4800	860	854
5000	887	887	5000	896	896

APPENDIX III

(Continued)

C. EVALUATION OF THE CALIBRATION CONSTANT.

Bolt BB-I:

5000 lb./885 microstrain = 5.65 lb. per microstrain, or

885 microstrain/5000 lb. = 0.178 microstrain per lb.

Bolt BB-II:

5000 lb./898 microstrain = 5.57 lb. per microstrain, or

898 microstrain/5000 lb. = 0.180 microstrain per lb.

Bolt BB-III:

5000 lb./887 microstrain = 5.64 lb. per microstrain, or

887 microstrain/5000 lb. = 0.177 microstrain per lb.

Bolt BB-IV:

5000 lb./896 microstrain = 5.58 lb. per microstrain, or

896 microstrain/5000 lb. = 0.179 microstrain per lb.

Average value: 5.61 lb. per microstrain $\pm$ 0.2 %.

APPENDIX IV

RECORD OF STATIC STRAIN READINGS.

Shot No.	Time (hours)	Blast-hole	Strain Readings from Bolts		
			Bolt BB-I	Bolt BB-II	Bolt BB-IV
	1st Day:		Instal-lation:		
	10.55		698	--	--
	11.40		674	--	--
1	12.30	BH-I	Photograph No. 1		
	13.30		658	--	--
2	15.00	BH-I	Photograph No. 4		
	15.07		645	--	--
3	16.00	BH-III	Photograph No. 7		
	16.30		631	--	--
	5th Day:			Instal-lation:	Instal-lation:
	10.25		615		
	10.40			698	
	10.55				698
	11.20				667
	11.22			684	
	11.24		612		
4	11.55	BH-III	Photographs No. 10, 11, 12.		
	12.09		576		
	12.12			672	
	12.14				652
	13.13				545
	13.15			669	
	13.17		570		
5	13.45	BH-III	Photographs No. 13, 14, 15.		
	13.55				641
	13.58			665	
	14.00		560		
6	14.20	BH-III	Photographs No. 16, 17, 18.		
	14.37				640
	14.40			659	
	14.43		551		
7	15.00	BH-III	Photographs No. 19, 20, 21.		
	15.18				635
	15.20			657	
	15.22		545		
8	15.45	BH-III	Photographs No. 22, 23, 24.		
	15.58				633
	15.59			653	
	16.00		527		
9	16.15	BH-III	Photographs No. 25, 26, 27.		
	16.32				630
	16.34			651	
	16.35		525		

APPENDIX IV

(Continued)

Shot No.	Time (hours)	Blast-hole	Strain Readings from Bolts: Bolt BB-I	Bolt BB-II	Bolt BB-IV
10	16.45	BH-II	Photographs No. 28, 29, 30.		
	17.00				530
	17.02			650	
	17.03		521		
	6th Day:				
	13.04				528
	13.10			647	
	13.13		470		
11	13.45	BH-III	Photographs No. 31, 32, 33.		
	14.17				526
	14.22			642	
	14.25		470		
12	14.45	BH-II	Photographs No. 34, 35, 36.		
	15.01				525
	15.04			640	
	15.06		465		
13	15.20	BH-I	Photographs No. 37, 38, 39.		
	15.40				523
	15.45			637	
	15.48		460 Dis-mounted.		
	8th Day:				
	11.59				515
	12.02			629	
14	12.30	BH-III	Photographs No. 40, 41, 42.		
	12.45				519
	12.47			624	
15	13.10	BH-I & BH-III	Photographs No. 43, 44, 45.		
	13.26				515
	13.29			621	
16	13.55	BH-I & BH-II & BH-III	Photographs No. 46, 47, 48.		
	14.26				510
	14.28			615	
17	14.50	BH-I & BH-II & BH-III	Photographs No. 49, 50, 51.		
	15.23				509
	15.26			612	
			Installation of Bolt BB-III:		
	12th Day:				
	9.33		708		
	9.35				505
	9.38			587	

APPENDIX IV

(Continued)

Shot No.	Time (hours)	Blast-hole	Strain Readings from Bolts: Bolt BB-III	Bolt BB-II	Bolt BB-IV
18	10.09	BH-I	Photographs No. 52, 53, 54.		
	10.33				505
	10.35			577	
	10.38		705		
19	11.09	BH-I & BH-III	Photographs No. 55, 56, 57.		
	12.10				500
	12.11			557	
	12.14		706		
20	12.35	BH-I & BH-III	Photographs No. 58, 59, 60.		
	12.58				498
	13.03			522	
	13.05		699		
21	13.20	BH-I & BH-III	Photographs No. 61, 62, 63.		
	13.43				496
	13.45			516	
	13.48		687		
22	14.10	BH-I	Photographs No. 64, 65, 66.		
	14.22				344
	14.25			436	
	14.27		675		
	15th Day:				
	12.22		657		
	12.25			470	
	12.27				492
23	13.04	BH-I	Photographs No. 67, 68, 69.		
	13.19				485
	13.21			461	
	13.23		642		
24	13.40	BH-I	Photographs No. 70, 71, 72.		
	13.56				480
	13.58			454	
	14.00		624		
	16th Day:				
	9.17				476
	9.20			448	
	9.24		623		
25	9.45	BH-I	Photographs No. 73, 74, 75.		
	9.56				474
	9.59			442	
	10.01		609		
26	10.15	BH-II	Photographs No. 76, 77, 78.		
	10.32				470

APPENDIX IV

(Continued)

Shot No.	Time (hours)	Blast-hole	Strain Readings from Bolts		
			Bolt BB-III	Bolt BB-II	Bolt BB-IV
	10.34			439	
	10.36		603		
27	10.50	BH-III	Photographs No. 79, 80, 81.		
	11.03				461
	11.05			435	
	11.07		599		
28	11.20	BH-II & BH-III	Photographs No. 82, 83, 84.		
	11.35				457
	11.36			427	
	11.38		596		
29	11.55	BH-IV	Photographs No. 85, 86, 87.		
	12.07				453
	12.08			418	
	12.10		569		
30	12.30	BH-IV & BH-I	Photographs No. 88, 89, 90.		
	12.39				448
	12.40			413	
	12.42		558		
32nd	Day:				
	15.00				426
	15.09			274	Dismounted.
	15.10		409 Dismounted.	Dismounted.	

APPENDIX V

RECORDING-EQUIPMENT OPERATING-DATA.

Shot No.	Transducer Current (ma) Trace Sensitivity (vertical) (mv/cm) Horizontal Sweep (ms/cm)				
	SENSORS				
	RG-I	RG-A	Bolt BB-I	Bolt BB-II	Bolt BB-IV
1	25 0.02 1	Not employ-	25 0.20 5	Not employ-ed	Not employ-ed
2	25 0.5 2	25 0.02 5	25 0.05 5	-"-	-"-
3	25 0.05 2	25 0.05 5	25 0.05 5	-"-	-"-
4	25 0.10 2	25 0.05 5	25 0.05 5	25 0.05 5	25 0.05 5
5	25 0.10 1	25 0.50 5	25 0.05 2	25 0.05 2	24 0.05 5
6	25 0.10 1	25 0.50 5	25 0.05 5	25 0.05 5	25 0.05 5
7	25 0.10 1	25 0.50 5	25 0.05 5	25 0.05 5	25 0.05 5
8	25 0.10 1	24 0.50 2	25 0.05 5	25 0.05 5	25 0.05 5
9	25 0.10 1	25 0.50 2	25 0.05 5	25 0.05 5	25 0.05 2
10	25 0.10 1	25 0.50 2	25 0.05 5	25 0.05 5	25 0.20 2

APPENDIX V

(Continued)

Shot No.	Transducer Current (ma) Trace Sensitivity (vertical) (mv/cm) Horizontal Sweep (ms/cm)				
			SENSORS		
	RG-I	RG-A	Bolt BB-I	Bolt BB-II	Bolt BB-IV
11	25 0.20 1	25 0.50 2	25 0.05 2	25 0.05 2	25 0.20 2
12	25 0.20 1	25 0.50 2	25 0.05 2	25 0.05 2	25 0.20 2
13	24 0.20 1	24 0.50 2	24 0.05 2	24 0.05 2	25 0.20 2
			Dismounted.		
14	25 0.50 1	25 0.20 2		25 0.05 2	25 0.10 2
15	25 0.50 1	25 0.10 2		25 0.05 2	25 0.10 2
16	25 0.50 1	25 0.10 2		25 0.05 2	25 0.10 2
17	25 0.50 1	25 0.10 2		25 0.05 2	25 0.10 2
			Remounted: Bolt BB-III		
18	25 0.50 1	25 0.50 2	25 0.05 2	25 0.05 2	25 0.05 2
19	25 0.50 2	25 0.20 2	25 0.05 2	— — —	25 0.05 2
20	25 0.50 1	25 0.20 2	25 0.05 2	25 0.05 2	25 0.05 2

APPENDIX V

(Continued)

Shot No.	Transducer Current (ma) Trace Sensitivity (vertical) (mv/cm) Horizontal Sweep (ms/cm)				
	SENSORS				
	RG-I	RG-A	Bolt BB-III	Bolt BB-II	Bolt BB-IV
21	24 0.50 5	24 0.20 5	24 0.02 5	24 0.02 5	24 0.02 5
22	25 0.50 5	24 0.20 1	24 0.05 2	24 0.05 2	24 0.02 1
23	25 0.50 5	25 0.20 1	25 0.05 2	25 0.05 2	25 0.02 1
24	25 0.50 2	25 0.20 1	25 0.05 2	25 0.05 2	25 0.01 1
25	25 0.50 2	25 0.20 1	25 0.05 2	25 0.05 2	25 0.02 1
26	25 0.50 2	25 0.20 1	25 0.05 2	25 0.05 2	25 0.02 1
27	25 0.50 2	25 0.20 1	25 0.05 2	25 0.05 2	25 0.02 1
28	25 0.50 2	25 0.20 1	25 0.05 2	25 0.05 2	25 0.02 1
29	25 0.50 2	25 0.20 1	25 0.05 2	25 0.05 2	25 0.02 1
30	25 2.00 2	25 0.50 1	25 0.20 2	25 0.20 2	25 0.02 1

APPENDIX VI

EVALUATION OF PEAK-STRAINS FROM OSCILLOSCOPE-TRACES.

The peak-strains determined by the investigation were computed from the following formula (21):

$$\varepsilon_p = dE\ (R_g+R_s)/S_m\ R_g\ R_s\ I\ , \qquad 7.$$

where ε_p = the peak strain-deflection (microstrain),

R_g = 495 ohm,

R_s = 3 100 ohm,

S_m = 3.46,

I = the current in milliamps listed in data record of Appendix V,

dE = the voltage output in mv, as determined from the peak amplitudes of the traces in cm and the vertical trace-sensitivities in mv/cm, also listed in Appendix V. The trace-amplitudes were read directly from the photographs, where the distance between the grid lines represented the length of 1 cm, as used for this interpretation.

Example: The response of Rock Sensor RG-I for Shot No. 3 in Appendix VI gave

$$dE = 3.00\ cm * 0.50\ mv/cm = \underline{1.50\ mv}.$$

Therefore, the peak strain-amplitude had

ε_p=1.50 mv*(495+3100) ohm / 3.46 * 495 ohm*3100 ohm*0.25 ma=<u>4.08 micro - strain</u>.

Peak strains for all tests are included in the tables that follow:

APPENDIX VI

(Continued)

A. Rock Sensors:

Shot No.	Photograph No.	SENSORS RG-I Trace Peak-Amplitude (cm)	RG-I Peak-Strain (microstrain)	RG-A Trace Peak-Amplitude (cm)	RG-A Peak-Strain (microstrain)
1	No traces gained				
2	No traces gained				
3	9	3.00	4.08	No traces gained	
4	12	4.00	10.80	No traces gained	
5	14	No traces gained		0.40	5.45
6	17	No traces gained		0.45	6.13
7	21 & 20	3.12	8.16	0.10	1.36
8	24 & 23	3.97	10.88	0.68	9.30
9	27 & 26	4.50	12.23	0.81	11.00
10	30	3.00	18.16	No traces gained	
11	33 & 32	3.00	16.40	0.35	4.80
12	36 & 35	1.70	9.26	0.35	4.80
13	39 & 38	4.00	22.70	0.50	6.81
14	42 & 41	1.30	17.70	1.10	6.00
15*	45 & 44	2.00	27.20	0.90	2.45
16*	48 & 47	No traces gained		1.00	2.72
17*	51 & 50	0.15	2.02	0.60	1.63
18	54 & 53	2.20	30.00	0.60	8.17
19*	57 & 56	No traces gained		0.30	1.64
20*	60 & 59	3.20	43.60	0.40	2.18
21*	63 & 62	1.00	13.60	0.92	5.22
22	66 & 65	1.60	21.80	0.70	3.99
23	69 & 68	2.55	34.50	0.80	4.36
24	72 & 71	2.80	38.10	0.30	16.35
25	75 & 74	3.50	47.70	0.80	4.36
26	78 & 77	1.50	20.40	0.91	4.94
27	81 & 80	1.00	13.60	0.60	3.27
28*	84 & 83	1.30	17.70	0.91	4.94
29	87 & 86	4.73	64.40	4.00	21.80
30*	90 & 89	0.67	36.50	0.80	10.90

Note: * indicates test shots made with multiple charges.

APPENDIX VI

(Continued)

B. Bolt Sensors:

Shot No.	Photograph No.	SENSORS Bolt BB-I Trace Peak-Amplitude (cm)	Bolt BB-I Peak-Strain (micro-strain)	Bolt BB-II Trace Peak-Amplitude (cm)	Bolt BB-II Peak-Strain (micro-strain)	Bolt BB-IV Trace Peak-Amplitude (cm)	Bolt BB-IV Peak-Strain (micro-strain)
1	No traces gained						
2	4	0.60	0.82	No traces gained			
3	7	0.40	0.55	No traces gained			
4	10 & 11	0.20	0.27	0.20	0.27	No traces gained	
5	13 & 14	No traces gained				0.40	0.56
6	16 & 17	0.18	0.24	0.20	0.27	0.80	1.09
7	19 & 20	0.12	0.16	0.12	0.16	0.92	1.25
8	22 & 23	0.07	0.10	0.10	0.13	0.70	0.95
9	25 & 26		No traces gained			0.80	1.09
10	28 & 29	0.20	0.27	0.20	0.27	0.33	1.80
11	31 & 32	0.16	0.22	0.16	0.22	0.15	0.82
12	34 & 35	0.15	0.20	0.15	0.20	0.18	0.98
13	37 & 38	0.30	0.41	0.18	0.25	0.25	1.35
Bolt BB-I substituted by Bolt BB-III:							
14	40 & 41	0.40	0.54	0.36	0.49	No traces gained	
15*	43 & 44	0.10	0.14	0.30	0.41	0.10	0.27
16*	46 & 47	0.10	0.14	0.15	0.20	0.60	1.63
17*	49 & 50	0.18	0.25	0.30	0.41	0.60	1.63
18	52 & 53	0.60	0.82	0.29	0.40	0.15	0.20
19*	55 & 56	0.20	0.27	No traces gained		0.10	0.14
20*	58 & 59	0.30	0.41	0.28	0.38	0.10	0.14
21*	61 & 62	0.51	0.72	0.73	0.41	0.30	0.17
22	64 & 65	0.52	0.74	0.30	0.43	0.40	0.23
23	67 & 68	0.41	0.56	0.29	0.40	0.20	0.11
24	70 & 71	0.41	0.56	0.25	0.34	1.00	0.27
25	73 & 74	0.37	0.50	0.13	0.18	0.30	0.16
26	76 & 77	0.30	0.41	0.60	0.82	0.40	0.22
27	79 & 80	0.20	0.27	0.30	0.41	0.25	0.14
28*	82 & 83	0.20	0.27	0.50	0.68	0.01	0.01
29	85 & 86	2.00	2.72	0.40	0.54	0.01	0.01
30*	88 & 89	0.20	1.10	0.30	1.64	0.40	0.22

Note: * indicates test shots with multiple charges.

APPENDIX VII

EXTRAPOLATION OF DYNAMIC PEAK-STRAINS AND COMPUTATION OF ENERGY OF ROCK-VIBRATION.

A. Formula for Peak-Strain Extrapolation.

If a strain amplitude decays according to the law (21)

$$\varepsilon_{pr} = (K/r)\ e^{-cr}, \qquad 8.$$

it will have the amplitude ε_{pr} at the distance r and the amplitude ε_{px} at the distance x from the shock source. If r is the distance from the shock source to the rock sensor and x is the distance from the shock source to a bolt sensor, the equations pertinent to those distances can be divided one by the other:

$$\frac{\varepsilon_{px}}{\varepsilon_{pr}} = \frac{(K/x)\ e^{-cx}}{(K/r)\ e^{-cr}} .$$

Therefore we can solve for the strain amplitude in the rock at a bolt location, x, in terms of the amplitude measured at a rock sensor and the coordinated travel distances:

$$\varepsilon_{px} = \varepsilon_{pr}\frac{r}{x}\ e^{c(r-x)} . \qquad 9.$$

The value of ε_{pr} in this equation is equivalent to the value of ε_{p} in Equation 7.

Example: For Shot No. 3, the strain amplitude in the rock at the location of Bolt BB-I, as a function of the amplitude recorded by the Rock Sensor RG-I, was

$$\varepsilon_{px} = 4.08\left(\frac{21.2}{21.8}\right)2.27^{0.026(21.2-21.8)} = \underline{3.90 \text{ microstrain}}.$$

APPENDIX VII

(Continued)

B. Determination of the Spring-Stiffness, S_r, for the Energy Evaluation.

One can calculate the Spring Stiffness for any material, from Hooke's Law. The force, S_r, necessary to strain a cylindrical body of a 1-in. length and 3/4-in. diameter for the amount of 1 microstrain in the axial direction would be as follows:

If

$$\sigma = \varepsilon E, \qquad 10.$$

then

$$S_r = \sigma a = \varepsilon E a. \qquad 11.$$

Since the Young's Modulus, E, for the rock was 5×10^6 psi, and the cross-sectional area, a, was 0.441 $in.^2$, we obtain

$$S_r = 3.5 \times 10^6 (0.441 \times 10^6) \times 1 = \underline{1.55 \times 10^{-6} \text{ lb./microstrain}}.$$

C. Calculation of Vibrational Energy, E_r, in the Rock.

The vibrational energy in the rock medium was calculated by applying Equation 5. By substituting into this equation the numerical values of ε_{pr} observed at the Rock Sensor RG-I and the numerical values of ε_{px} as obtained from Equation 9., the energy of vibration, E_r, was computed for the location of RG-I and for each of the bolt locations, respectively. Pertinent data are included in the accompanying tables.

APPENDIX VII

(C. Continued)

Shot No.	Blasthole No.	Bolt Position	ε_{pr}	r	x	c(r-x)	$e^{c(r-x)}$	ε_{px}	E_r (in-lbs x 10^{-6})
3	BH-III		4.08	21.2					12.9
		BB-I			21.8	-0.016	0.983	3.90	11.8
		BB-II			24.2	-0.078	0.924	3.29	8.4
		BB-IV			27.8	-0.173	0.840	2.60	5.2
4	BH-III		10.80	21.2					83.9
		BB-I			21.8	-0.016	0.983	10.32	80.0
		BB-II			24.2	-0.078	0.924	8.74	59.0
		BB-IV			27.8	-0.173	0.840	6.91	37.0
5	BH-III	No data gained							
6	BH-III		8.99	21.2					62.6
		BB-I			21.8	-0.016	0.983	8.60	57.4
		BB-II			24.2	-0.078	0.924	7.27	41.0
		BB-IV			27.8	-0.173	0.840	5.76	25.7
7	BH-III		8.49	21.2					55.8
		BB-I			21.8	-0.016	0.983	8.11	51.1
		BB-II			24.2	-0.078	0.924	6.87	36.7
		BB-IV			27.8	-0.173	0.840	5.44	22.9
8	BH-III		10.88	21.2					84.5
		BB-I			21.8	-0.016	0.983	10.40	80.6
		BB-II			24.2	-0.078	0.924	8.80	69.8
		BB-IV			27.8	-0.173	0.840	6.96	37.6
9	BH-III		12.23	21.2					116.0
		BB-I			21.8	-0.016	0.983	11.70	106.1
		BB-II			24.2	-0.078	0.924	9.90	77.0
		BB-IV			27.8	-0.173	0.840	7.84	47.7
10	BH-I		8.16	13.2					51.6
		BB-I			14.0	-0.021	0.980	7.55	26.5
		BB-II			19.3	-0.159	0.854	4.77	17.6
		BB-IV			22.4	-0.257	0.779	3.75	10.9
11	BH-III		16.40	21.2					216.0
		BB-I			21.8	-0.016	0.983	15.67	190.0
		BB-II			24.2	-0.078	0.924	13.28	136.5
		BB-IV			27.8	-0.173	0.840	10.50	81.5

APPENDIX VII

(C. Continued)

Shot No.	Blasthole No.	Bolt Position	ε_{pr}	r	x	c(r-x)	$e^{c(r-x)}$	ε_{px}	E_r (in.-lb. x 10^{-6})
12	BH-III		9.26	13.2					66.0
		BB-I			14.0	-0.021	0.980	8.55	56.6
		BB-II			19.3	-0.159	0.854	5.41	22.7
		BB-IV			22.4	-0.247	0.779	4.24	14.0
13	BH-II		22.70	9.5					400.0
		BB-I			10.2	-0.018	0.980	20.70	332.0
		BB-II			13.2	-0.096	0.906	14.80	170.0
		BB-IV			16.6	-0.158	0.830	10.80	83.6
14	BH-III		17.70	21.2					243.0
		BB-III			21.8	-0.016	0.983	16.90	222.0
		BB-II			24.2	-0.078	0.924	14.32	159.0
		BB-IV			27.8	-0.173	0.840	11.30	99.4
18	BH-II		30.00	9.5					698.0
		BB-III			10.2	-0.018	0.980	27.40	581.0
		BB-II			13.2	-0.096	0.906	19.55	269.0
		BB-IV			16.6	-0.158	0.830	14.20	156.0
22	BH-II		21.80	9.5					368.0
		BB-III			10.2	-0.018	0.980	19.90	307.0
		BB-II			13.2	-0.096	0.906	14.20	156.0
		BB-IV			16.6	-0.185	0.830	10.40	81.0
23	BH-II		34.5	9.5					922.0
		BB-III			10.2	-0.018	0.980	31.50	768.0
		BB-II			13.2	-0.096	0.906	22.50	396.0
		BB-IV			16.6	-0.185	0.830	16.36	208.2
24	BH-II		38.10	9.5					1124.0
		BB-III			10.2	-0.018	0.980	34.80	935.0
		BB-II			13.2	-0.096	0.906	24.80	476.0
		BB-IV			16.6	-0.185	0.830	18.61	268.0
25	BH-II		47.70	9.5					1768.0
		BB-III			10.2	-0.018	0.980	43.60	1471.0
		BB-II			13.2	-0.096	0.906	31.00	744.0
		BB-IV			16.6	-0.185	0.830	22.60	395.0
26	BH-I		20.40	13.2					322.0
		BB-III			14.0	-0.021	0.980	20.10	312.0
		BB-II			19.2	-0.159	0.854	11.90	109.7
		BB-IV			22.4	-0.247	0.779	9.34	67.5

APPENDIX VII

(C. Continued)

Shot No.	Blasthole No.	Bolt Position	ε_{pr}	r	x	c(r-x)	$e^{c(r-x)}$	ε_{px}	E_r (in.-lb. x 10^{-6})
27	BH-III		13.60	21.2					143.1
		BB-III			21.8	-0.016	0.983	13.00	131.0
		BB-II			24.2	-0.078	0.924	11.00	93.5
		BB-IV			27.8	-0.173	0.840	8.70	50.9

APPENDIX VIII

COMPUTATION OF ENERGY OF BOLT-VIBRATION.

A. Determination of the Spring Stiffness, S_b, for Bolts.

As was done in Appendix VII, B., the body size and shape of a bolt element of 1-in. length was taken as reference for the evaluation of the vibrational energy. Using a Young's Modulus for steel rock-bolts of 3.2×10^7 psi, we obtain

$$S_b = 3.2 \times 10^7 \times (0.441 \times 10^{-6}) \times 1 = \underline{14.13 \times 10^{-6} \text{ lb./microstrain}}.$$

B. Calculation of Vibrational Energy, E_b, in Bolts.

For computation of vibrational energies in the bolt sensors, Equation 5 was adjusted by substituting the numerical values of ϵ_p, i.e., the peak strain amplitudes recorded from the bolt sensors, and by use of the value for S_b as calculated above. The results are listed below:

Shot No.	Blasthole No.	BOLT SENSOR Bolt BB-I		Bolt BB-II		Bolt BB-IV	
		ϵ_p	E_b	ϵ_p	E_b	ϵ_p	E_b
2	BH-II	0.82	4.75	--	--	--	--
3	BH-III	0.55	2.12	--	--	--	--
4	BH-III	0.27	0.53	0.27	0.52	--	--
5	BH-III	--	--	--	--	0.56	2.26
6	BH-III	0.24	0.41	0.27	0.52	1.09	8.22
7	BH-III	0.16	0.18	0.16	0.18	1.25	11.05
8	BH-III	0.11	0.07	0.14	0.14	0.95	6.44
9	BH-III	--	--	--	--	1.09	8.22
10	BH-I	0.27	0.52	0.27	0.52	1.80	22.30
11	BH-III	0.22	0.34	0.21	0.33	0.82	4.65
12	BH-I	0.20	0.31	0.20	0.31	0.98	6.80
13	BH-II	0.14	1.17	0.25	0.43	1.35	12.83
Bolt BB-III substituted for BB-I:							
14	BH-III	0.54	2.05	0.49	1.70	--	--
18	BH-II	0.82	4.52	0.40	1.17	0.20	0.30
22	BH-II	0.74	3.88	0.43	1.31	0.23	0.38
23	BH-II	0.56	2.20	0.40	1.17	0.11	0.08
24	BH-II	0.56	2.20	0.34	0.82	0.27	0.52
25	BH-II	0.50	1.79	0.18	0.22	0.16	0.18
26	BH-I	0.41	1.17	0.82	4.50	0.22	0.34
27	BH-III	0.27	0.52	0.41	1.18	0.14	0.14

Note: E_b stands for the vibrational energy with the dimension in-lb.$\times 10^{-6}$.

REFERENCES.

1. STEFANKO, R., and DE LA CRUZ, R.V. (1964). Mechanism of Load Loss in Roof Bolts. Sixth Symposium on Rock Mechanics, University of Missouri at Rolla, Proceedings.

2. BURCHELL, H.J. (1955). Rock Bolting. Canadian Mining and Metallurgical Bulletin, Vol.LVIII, Oct.

3. HOLLAND, C.T., and WOJCIECHOWSKI, J.J. (1956). Some Aspects of Roof Bolt Action in a Coal Mine Roof. Mineral Industry Journal, Vol.3, No.4, Dec.

4. PANEK, L.A. (1955). Analysis of Roof Bolt Systems Based on Model Studies. Mining Engineering, Vol.7, No.10, Oct.

5. SCHMUCK, H.K. (1957). Theory and Practice of Rock Bolting. The Colorado School of Mines Quarterly, Vol.52, No.3, July.

6. THOMAS, E. (1954). Rock Bolting Finds Wide Application. Mining Engineering, Vol.6, No.11, Nov.

7. SCHMUCK, H.K. (1956). How Western Mines Use Metallic Fabric Lagging for Support Between Bolts. Mining World, Vol.18, No.12, Nov.

8. BRECKENRIDGE, R.N., and POLLISH, L. (1954). Rock Bolting in Metal Mines of the Northwest. Mining Engineering, Vol.6, No.7, July.

9. PANEK, L.A. (1957). Anchorage Characteristics of Rock Bolts. Mining Congress Journal, Vol.43, No.11, Nov.

10. STEFANKO, R. (1962). New Look at Long Term Anchorage: Key to Roof Bolt Efficiency. Mining Engineering, Vol.14, No.5, May.

11. LANG, T.A. (1961). Theory and Practice of Rock Bolting. AIME Transactions - Mining, Vol.220, Feb.

12. HOEVELS, W., and ROLSHOVEN, H. (1952). Betriebsversuche mit Ankerausbau auf dem Steinkohlenbergwerk Consolidation unter Beruecksichtigung amerikanischer Erfahrungen. Glueckauf, Heft 13/14.

13. JACOBI, O., and MIDDENDORF, W. (1952). Ankerausbau in Abbaustrekken. Glueckauf, Heft 25/26.

14. MAHOOD, G.P., DEMPSEY, J.B., ROBERTSON, A.B., SANFORD, J.H., and THOMAS, E.M. (1956). Specifications of Roof Bolting Materials. Mining Congress Journal, Vol.42, No.7, July.

15. . . . . (1959). Standard Roof Bolt Anchorage Testing Procedure. Mining Congress Journal, Vol.45, No.12, Dec.

16. SCOTT, J.J. (1964). Personal Communication.

17. ASH, R.L. (1964). Personal Communication.

18. DE LA CRUZ, R.V. (1964). Mechanism of Bolt Anchorage. M.S. Thesis, The Pennsylvania State University.

19. DUVALL, W.J., and OBERT, L. (1949). A Gage and Recording Equipment for Measuring Dynamic Strains in Rock. USBM, RI-4581.

20. DUVALL, W.J. (1953). Strain Waves in Rock Near Explosions. Geophysics, Vol.18, No.2, April.

21. QUAN, C.K. (1964). The Characteristics of Radial Strain Propagation Induced by Explosives Impact in Jefferson City Dolomite. M.S. Thesis, The University of Missouri at Rolla.

22. CAUDLE, R.D. (1962). Experiments on the Measurement of the Response of Rock to Dynamic Loads. M.S. Thesis, The University of Missouri at Rolla.

23. ASH, R.L. (1965). The Influence of Petrofabrics on Blasting Effects. Paper presented at Annual Meeting of AIME, Chicago, Feb.

24. BULLEN, K.E. (1959). Introduction to Theory of Seismology. Cambridge University Press, Cambridge, England.

25. FREY, A.R., and KINSLER, L.E. (1961). Fundamentals of Accoustics. J. Wiley, New York.

26. GROSSLEY, F.R.E. (1954). Dynamics in Machines. The Ronald Press Company, New York.

27. STEHLIK, Ch.J. (1964). Mine Roof Rock and Roof Bolt Behavior Resulting from Nearby Blasts. USBM, RI-6372.

28. HARTMAN, H.L., and TANDANAND, S. (1962). Investigation of Dynamic Failure by High Speed Photography. Fifth Symposium on Rock Mechanics at the University of Minnesota, Proceedings.

VITA.

Helmut W. Habenicht was born on December 24, 1937, in Klagenfurt, Austria. A citizen of Austria, he received the major part of his education in that Country. He attended the elementary schools in Pattergassen and Millstatt and the highschool Bundesrealgymnasium Spittal in Spittal/Drau. After graduation in 1956, he continued his studies in the mining fields at the Montanistische Hochschule Leoben. He was awarded the degree of Diplom-Ingenieur in Mining Engineering in December 1961 and that of Diplom-Ingenieur in Petroleum Engineering in April 1963. Along with his college education he worked part time to gain practical experience in surface and underground mining of coal, iron, copper, magnesite, gold, and petroleum.

In September 1963, he received a Graduate Assistantship from the Department of Mining Engineering of the University of Missouri at Rolla, Missouri, which enabled him to engage in advanced studies with an emphasis on blasting techniques and rock mechanics.

During this latter period, he was accepted as a member of AIME and of Sigma Gamma Epsilon.